

Optimal SIC Ordering and Power Allocation in Downlink Multi-Cell NOMA Systems

Sepehr Rezvani, Eduard A. Jorswieck, *Fellow, IEEE*, Nader Mokari, *Senior Member, IEEE*, and Mohammad R. Javan, *Senior Member, IEEE*

Abstract

In this work, we consider the problem of finding globally optimal joint successive interference cancellation (SIC) ordering and power allocation (JSPA) for the general sum-rate maximization problem in downlink multi-cell NOMA systems. We propose a globally optimal solution based on the exploration of base stations (BSs) power consumption and distributed power allocation. The proposed centralized algorithm is still exponential in the number of BSs, however scales well with larger number of users. For any suboptimal decoding order, we address the problem of joint rate and power allocation (JRPA) to achieve maximum users sum-rate. Furthermore, we design semi-centralized and distributed JSPA frameworks with polynomial time complexity. Numerical results show that the optimal decoding order results in significant performance gains in terms of outage probability and users total spectral efficiency compared to the channel-to-noise ratio (CNR)-based decoding order known from single-cell NOMA. Moreover, it is shown that the performance gap between our proposed centralized and semi-centralized frameworks is quite low. Therefore, the low-complexity semi-centralized framework with near-to-optimal performance is a good choice for larger number of BSs and users.

Index Terms

Multi-cell, NOMA, successive interference cancellation, optimal SIC ordering, power allocation.

S. Rezvani and E. A. Jorswieck are with the Department of Information Theory and Communication Systems, Technische Universität Braunschweig, Braunschweig, Germany (e-mails: {rezvani, jorswieck}@ifn.ing.tu-bs.de).

N. Mokari is with the Department of Electrical and Computer Engineering, Tarbiat Modares University, Tehran, Iran (e-mail: nader.mokari@modares.ac.ir).

M. R. Javan is with the Department of Electrical and Robotics Engineering, Shahrood University of Technology, Shahrood, Iran (e-mail: javan@shahroodut.ac.ir).

I. INTRODUCTION

A. Motivations and Related Works

It is known that the channel capacity of degraded broadcast channels can be achieved by performing linear superposition coding (in power domain) at the transmitter side combined with multiuser detection algorithms, such as successive interference cancellation (SIC), at the receiver side [1], [2]. This technique is known as power-domain non-orthogonal multiple access (NOMA) which is considered as a new radio access technique for the fifth generation (5G) wireless networks and beyond [3]–[5]. In information theory, the main purpose of NOMA¹ is reducing the complexity of dirty paper coding (DPC) to attain the capacity region of degraded broadcast channels. According to the SIC of NOMA, the SIC decoding order among multiplexed users plays an important role to achieve the capacity region of degraded broadcast channels [6]–[8].

It is well-known that the downlink single-input single-output (SISO) Gaussian broadcast channels are degraded [1], [2]. Hence, NOMA with channel-to-noise ratio (CNR)-based decoding order is capacity achieving in SISO Gaussian broadcast channels meaning that any rate region is a subset of the rate region of NOMA with CNR-based decoding order [1], [2], [9]. The superiority of single-cell NOMA over single-cell OMA is also well-known in information theory [5], [6], [10]. In single-cell NOMA, it is verified that the power allocation optimization is necessary to achieve the maximum spectral efficiency of users [4]–[8]. From the optimization perspective, the optimal (CNR-based) decoding order is independent from the power allocation, so is robust and straightforward. Moreover, it is shown that the Hessian of sum-rate function under the CNR-based decoding order is strictly concave on powers [11]–[13]. In this way, the sum-rate maximization problem in downlink single-cell NOMA is convex². The latter convex problem can be efficiently solved by using the Lagrange dual method.

Unfortunately, the capacity-achieving schemes are unknown in downlink multi-cell networks, since the capacity region of the two-user downlink interference channel is still unknown in general [2], [6], [16]. In this work, we limit our study to the downlink single-antenna multi-cell network, where the signal of users who do not belong to the associated cell is fully treated as additive white Gaussian noise (AWGN), also called inter-cell interference (ICI) [17]–[28].

¹In this work, the term 'NOMA' is referred to power-domain NOMA.

²The feasible region of the general power allocation problem in single-cell NOMA under the quality of service (QoS) requirement constraints is affine, so is convex [11]–[15].

Inspired by the degradation of SISO Gaussian broadcast channels, NOMA with channel-to-interference-plus-noise ratio (CINR)-based decoding order has the same performance as DPC at each cell such that it achieves the channel capacity of this multi-cell network called multi-cell NOMA. In this system, 'ICI+AWGN' can be viewed as equivalent noise power at the users. In contrast to single-cell NOMA, finding optimal decoding order in multi-cell NOMA is challenging, because of the impact of ICI on the CINR of multiplexed users [18], [19], [22], [24]–[28]. The ICI at each cell is affected by the total power consumption of each neighboring (interfering) base station (BS). Therefore, the optimal SIC decoding order in each cell depends on the optimal power consumption of all the other interfering BSs. As a result, the optimal SIC decoding order in each cell should be jointly determined with centralized power allocation optimization in all the neighboring cells. It is shown that under the CINR-based decoding order, the ICI in the centralized total power minimization problem verifies the basic properties of the standard interference function [18], [22], [25]. Hence, the optimal joint SIC ordering and power allocation (JSPA) can be obtained by using the well-known Yates power control framework [17]. In other words, the globally optimal JSPA for total power minimization problem in multi-cell NOMA can be found in an iterative distributed manner with a fast convergence speed [18], [21], [22], [25]. However, the ICI in the centralized sum-rate maximization problem does not verify the basic properties of the standard interference function. As a result, Yates power control framework does not guarantee any global optimality for the sum-rate maximization problem [25]. It is shown that the sum-rate function in multi-cell NOMA is nonconcave in powers, due to existing ICI, which makes the centralized sum-rate maximization problem nonconvex and strongly NP-hard [23]–[26]. The best candidate solution for solving this problem is monotonic optimization which is still approximately exponential in the number of users [23], [29]. The JSPA needs to examine the monotonic-based power allocation $(M!)^B$ times, where $(M!)^B$ is the total number of possible decoding orders in B cells each having M users. Therefore, the joint optimization via the monotonic optimization is basically impractical even at lower number of BSs and users. In [23], [25], the authors address the sum-rate maximization problem in multi-cell NOMA for the CNR-based decoding order resulting in suboptimal performance. In [24], [26], the SIC decoding orders are updated at the NOMA clustering subproblem, where the power allocation is fixed. And, the centralized power allocation subproblem is solved according to the fixed decoding orders. Since the optimal decoding order inherently depends on ICI, the

latter schemes cannot guarantee any global optimality³, meaning that NOMA results in a lower performance than the DPC. To the best of our knowledge, the optimal JSPA for maximizing users sum-rate in downlink multi-cell NOMA systems is still an open problem. Moreover, the performance gap between the optimal and suboptimal decoding orders in multi-cell NOMA is not yet addressed in the literature.

B. Our Contributions

In this work, we study the fundamentals of optimal/suboptimal decoding orders on the capacity region of the downlink multi-cell NOMA system including a single (fixed) NOMA cluster [1], [2], [18] in each cell⁴. Our main contributions are presented as follows:

- We study the fundamentals of SIC in multi-cell NOMA systems. By analyzing the Karush-Kuhn-Tucker (KKT) optimality conditions, we prove that at any feasible power consumption level of BSs, only the NOMA cluster-head user⁵ determined by adaptive (optimal) SIC decoding order deserves additional power, while the users with lower decoding order get power to only maintain their individual minimal rate demands. Then, we obtain closed-form expressions of the optimal power allocation and SIC ordering in multi-cell NOMA for the given BSs power consumption.
- We propose a globally optimal JSPA algorithm for maximizing users sum-rate under the individual minimum rate demand of users. This algorithm utilizes both the exploration of BSs power consumption and distributed power allocation. We show that this algorithm is a good solution for larger number of users while small number of BSs⁶.
- We analytically prove that under specific channel conditions, called SIC sufficient condition, the CNR-based decoding order is optimal for a user pair independent from power allocation.
- We analyze the impact of any suboptimal decoding order on the capacity region of multi-cell NOMA. In contrast to [20], [23]–[27], we show that under any fixed (thus suboptimal)

³Imposing the commonly-used SIC necessary condition in NOMA clustering among users would result a suboptimal performance. The global optimality can be guaranteed only if the optimal decoding orders be completely independent from ICI levels at all the cells for some channel conditions.

⁴In this work, we aim to investigate the impact of ICI on optimal decoding orders in sum-rate maximization problem which inherently depends on power allocation. Generalizing this model to multiple NOMA clusters within a cell is considered as a future work.

⁵The user with the highest decoding order which cancels the desired signal of all the other NOMA users within the cell.

⁶In practice, the number of interfering BSs is small anyway.

decoding order, joint rate and power allocation (JRPA) is necessary to achieve the channel capacity of users. For a suboptimal decoding order, we propose a near-to-optimal JRPA algorithm based on the sequential programming with polynomial complexity. The convergence and performance of the JRPA algorithm for different initialization methods are investigated. The SIC sufficient condition is utilized to reduce the complexity of the JRPA algorithm.

- We prove that under any suboptimal decoding order, guaranteeing successful SIC at all the users by imposing the commonly-used SIC necessary constraint on power allocation [23]–[27] may significantly degrade the total spectral efficiency of users.
- We also propose a globally optimal power allocation for any fixed (suboptimal) decoding order under the SIC necessary constraint by modifying our proposed JSPA algorithm.
- We propose a semi-centralized framework for a two-tier heterogeneous network (HetNet) consisting of multiple femto BSs (FBSs) underlying a single macro BS (MBS). We numerically show that this framework has a near-to-optimal performance with significantly reduced complexity, so is a good solution for practical implementations.

C. Paper Organization

The rest of this paper is presented as follows. Section II describes the general multi-cell NOMA system, and formulates the JSPA problem for maximizing users sum-rate. The solution algorithms are presented in Section III. Numerical results are provided in Section IV. Our conclusions are presented in Section V.

II. GENERAL DOWNLINK MULTI-CELL NOMA SYSTEM

Consider the downlink transmission of a multi-user single-carrier multi-cell NOMA system. The set of single-antenna BSs, and users served by BS b are indicated by \mathcal{B} and \mathcal{U}_b , respectively. According to the NOMA protocol, the users associated to the same transmitter form a NOMA cluster. The signal of users associated to other transmitters (known as ICI) is fully treated as AWGN at users within the NOMA cluster. Hence, we consider a single NOMA cluster at each cell b [18] including $|\mathcal{U}_b|$ users, where $|\cdot|$ is the cardinality of a set. The term $k \rightarrow i$ indicates that user k has a higher decoding order than user i such that user k is scheduled (and enforced) to decode and cancel the whole signal of user i , while the whole signal of user k is treated as INI at user i . For instance, assume that each cell b serves M users, i.e., $|\mathcal{U}_b| = M$. Generally, there are $M!$ possible decoding orders for users within the M -order NOMA cluster.

Without loss of generality, let $k \rightarrow i$ if $k > i$, i.e., the SIC of NOMA in each cell b follows $M \rightarrow M-1 \rightarrow \dots \rightarrow 1$. As shown in Fig. 1 in [18], in this SIC decoding order, the signal of each user i will be decoded prior to user $k > i$. In general, each user i first decodes and cancels the signal of users $1, \dots, i-1$. Then, it decodes its desired signal such that the signal of users $i+1, \dots, M$ is treated as noise at user i [5]. In this regard, in each cell, the NOMA cluster-head user M does not experience any intra-NOMA interference (INI).

Let $s_{b,i} \sim \mathcal{CN}(0, 1)$ be the desired signal of user $i \in \mathcal{U}_b$. Denoted by $\lambda_{b,i,k} \in \{0, 1\}$, the binary decoding decision indicator, where $\lambda_{b,i,k} = 1$ if user $k \in \mathcal{U}_b$ is scheduled to decode (and cancel when $k \neq i$) $s_{b,i}$, and otherwise, $\lambda_{b,i,k} = 0$. Since for each user pair within a NOMA cluster only one user can decode and cancel the signal of other user, we have $\lambda_{b,i,k} + \lambda_{b,k,i} = 1$, $\forall b \in \mathcal{B}, i, k \in \mathcal{U}_b, k \neq i$. Moreover, the signal of each user should be decoded at that user, meaning that $\lambda_{b,i,i} = 1$, $\forall b \in \mathcal{B}, i \in \mathcal{U}_b$. Due to the transitive nature of SIC ordering, if $\lambda_{b,i,k} = 1$ and $\lambda_{b,k,h} = 1$, then we should have $\lambda_{b,i,h} = 1$. In other words, we have $\lambda_{b,i,k} \lambda_{b,k,h} \leq \lambda_{b,i,h}$, $\forall b \in \mathcal{B}, i, k, h \in \mathcal{U}_b$. According to the SIC protocol, $s_{b,i}$ should be decoded at user $i \in \mathcal{U}_b$ as well as all the users in⁷ $\Phi_{b,i} = \{k \in \mathcal{U}_b \setminus \{i\} \mid \lambda_{b,i,k} = 1\}$. Therefore, in the SIC of NOMA, each user i first decodes and subtracts each signal $s_{b,j}$, $\forall j \in \mathcal{U}_b \setminus \{i\} \cup \Phi_{b,i}$, then it decodes its desired signal $s_{b,i}$ such that the signal of users in $\Phi_{b,i}$ is treated as noise (called INI). According to the SIC protocol, the signal of user i will be decoded prior to user k if $|\Phi_{b,i}| > |\Phi_{b,k}|$. According to the above, the SIC decoding order among users can be determined by finding $\lambda_{b,i,k}$. Actually, $\lambda_{b,i,k} = 1$, $\forall b \in \mathcal{B}, i, k \in \mathcal{U}_b, k \neq i$ is equivalent to $k \rightarrow i$ in cell b . Similar to [11]–[14], [18]–[28], we assume that the perfect channel state information (CSI) of all the users is available at the scheduler. The channel gain from BS $j \in \mathcal{B}$ to user $i \in \mathcal{U}_b$ is denoted by $g_{j,b,i}$. The allocated power from BS b to user $i \in \mathcal{U}_b$ is denoted by $p_{b,i}$. After performing perfect SIC⁸ at each user $l \in \mathcal{U}_b \setminus \Phi_{b,i}$, the received signal of user $i \in \mathcal{U}_b$ at user $k \in \{i\} \cup \Phi_{b,i}$ is given by

$$y_{b,i,k} = \underbrace{\sqrt{p_{b,i}} g_{b,b,k} s_{b,i}}_{\text{intended signal}} + \underbrace{\sum_{j \in \Phi_{b,i}} \sqrt{p_{b,j}} g_{b,b,k} s_{b,j}}_{\text{INI}} + \underbrace{\sum_{\substack{j \in \mathcal{B} \\ j \neq b}} \sum_{l \in \mathcal{U}_j} \sqrt{p_{j,l}} g_{j,b,k} s_{j,l}}_{\text{ICI}} + N_{b,k}, \quad (1)$$

⁷The term $\Phi_{b,i}$ is the set of users in cell b with higher decoding orders than user $i \in \mathcal{U}_b$.

⁸In this work, we aim to address the performance gain of finding optimal decoding order and power allocation for maximizing users total spectral efficiency in multi-cell NOMA systems. Considering any imperfect SIC is considered as a future work.

where the first and second terms are the received desired signal and INI of user $i \in \mathcal{U}_b$ at user $k \in \mathcal{U}_b$, respectively. The third term represents the ICI at user $k \in \mathcal{U}_b$. Moreover, $N_{b,k}$ is the AWGN at user $k \in \mathcal{U}_b$ with zero mean and variance $\sigma_{b,k}^2$. Without loss of generality, assume that $|s_{b,i}| = 1$, $\forall b \in \mathcal{B}$, $i \in \mathcal{U}_b$, and $h_{j,b,k} = |g_{j,b,k}|^2$ [13], [18], [25]. According to (1), the SINR of user $k \in \Phi_{b,i}$ for decoding and canceling the signal of user $i \in \mathcal{U}_b$ is $\gamma_{b,i,k} = \frac{p_{b,i}h_{b,b,k}}{\sum_{j \in \Phi_{b,i}} p_{b,j}h_{b,b,k} + (I_{b,k} + \sigma_{b,k}^2)}$, where $\sum_{j \in \Phi_{b,i}} p_{b,j}h_{b,b,k}$ is the INI power of user $i \in \mathcal{U}_b$ (after perfect SIC) received at user $k \in \mathcal{U}_b$, and $I_{b,k} = \sum_{j \in \mathcal{B}} \sum_{l \in \mathcal{U}_j, l \neq b} p_{j,l}h_{j,b,k}$ is the received ICI power at user $k \in \mathcal{U}_b$. For the case that $k = i$, $\gamma_{b,i,i}$ denotes the SINR of user $i \in \mathcal{U}_b$ for decoding its desired signal $s_{b,i}$ after perfect SIC. For convenience, let $h_{b,b,i} \equiv h_{b,i}$, and $\gamma_{b,i,i} \equiv \gamma_{b,i}$. Furthermore, let us denote the matrix of all the decoding indicators by $\boldsymbol{\lambda} = [\lambda_{b,i,k}]$, $\forall b \in \mathcal{B}, i, k \in \mathcal{U}_b$, in which $\boldsymbol{\lambda}_b = [\lambda_{b,i,k}]$, $\forall i, k \in \mathcal{U}_b$, represents the decoding indicator matrix of users in \mathcal{U}_b . Moreover, \mathbf{p} is the matrix of power allocation among all the users, in which \mathbf{p}_b is the b -th row of this matrix indicating the power allocation vector of users in cell b . According to the Shannon's capacity formula, the achievable spectral efficiency of user $i \in \mathcal{U}_b$ can be obtained by [4], [5]

$$R_{b,i}(\mathbf{p}, \boldsymbol{\lambda}_b) = \min_{k \in \{i\} \cup \Phi_{b,i}} \left\{ \log_2 \left(1 + \frac{p_{b,i}h_{b,k}}{\sum_{j \in \Phi_{b,i}} p_{b,j}h_{b,k} + (I_{b,k}(\mathbf{p}_{-b}) + \sigma_{b,k}^2)} \right) \right\}. \quad (2)$$

Note that the set $\Phi_{b,i}$ depends on $\boldsymbol{\lambda}_b$, although it is not explicitly shown in (2). The centralized total spectral efficiency maximization problem is formulated by

$$\text{JSPA : } \max_{\mathbf{p} \geq 0, \boldsymbol{\lambda} \in \{0,1\}} \sum_{b \in \mathcal{B}} \sum_{i \in \mathcal{U}_b} R_{b,i}(\mathbf{p}, \boldsymbol{\lambda}_b) \quad (3a)$$

$$\text{s.t.} \quad \sum_{i \in \mathcal{U}_b} p_{b,i} \leq P_b^{\max}, \quad \forall b \in \mathcal{B}, \quad (3b)$$

$$R_{b,i}(\mathbf{p}, \boldsymbol{\lambda}_b) \geq R_{b,i}^{\min}, \quad \forall b \in \mathcal{B}, i \in \mathcal{U}_b, \quad (3c)$$

$$\lambda_{b,i,k} + \lambda_{b,k,i} = 1, \quad \forall b \in \mathcal{B}, i, k \in \mathcal{U}_b, k \neq i, \quad (3d)$$

$$\lambda_{b,i,k} \lambda_{b,k,h} \leq \lambda_{b,i,h}, \quad \forall b \in \mathcal{B}, i, k, h \in \mathcal{U}_b, \quad (3e)$$

$$\lambda_{b,i,i} = 1, \quad \forall b \in \mathcal{B}, i \in \mathcal{U}_b. \quad (3f)$$

where (3b) and (3c) are the per-BS maximum power and per-user minimum spectral efficiency constraints, respectively. P_b^{\max} denotes the maximum power of BS b , and $R_{b,i}^{\min}$ is the minimum spectral efficiency demand of user $i \in \mathcal{U}_b$. The rest of the constraints are described above.

III. SOLUTION ALGORITHMS FOR THE SUM-RATE MAXIMIZATION PROBLEM

In this section, we propose globally optimal and suboptimal solutions for the main problem (3) under the centralized/decentralized resource management frameworks. Finally, we compare the computational complexity of the proposed resource allocation algorithms.

A. Centralized Resource Management Framework

In this subsection, we first propose a globally optimal JSPA algorithm for problem (3). Then, by considering a fixed SIC decoding order in (3), we propose two suboptimal rate adoption and power allocation algorithms.

1) *Globally Optimal JSPA Algorithm*: Problem (3) can be classified as a mixed-integer nonlinear programming (MINLP) problem. The sum-rate function in (3a) is nonconcave in \mathbf{p} and $\boldsymbol{\lambda}$ which makes (3) nonconvex and strongly NP-hard [23], [25]. Let us define the power consumption coefficient of BS b as $\alpha_b \in [0, 1]$ such that $\sum_{i \in \mathcal{U}_b} p_{b,i} = \alpha_b P_b^{\max}$. The received ICI power at user $i \in \mathcal{U}_b$ can be reformulated by $I_{b,i}(\boldsymbol{\alpha}_{-b}) = \sum_{\substack{j \in \mathcal{B} \\ j \neq b}} \alpha_j P_j^{\max} h_{j,b,i}$. Let $\boldsymbol{\alpha} = [\alpha_b]_{1 \times B}$ be the BSs power coefficient vector. We prove that for any given $\boldsymbol{\alpha}_{-b}$, the optimal $(\boldsymbol{\lambda}_b^*, \mathbf{p}_b^*)$ can be obtained in closed form as follows:

Proposition III.1. *In multi-cell NOMA, the optimal decoding order for the user pair $i, k \in \mathcal{U}_b$ is $k \rightarrow i$ if and only if $\tilde{h}_{b,i}(\boldsymbol{\alpha}_{-b}) \leq \tilde{h}_{b,k}(\boldsymbol{\alpha}_{-b})$, where $\tilde{h}_{b,l}(\boldsymbol{\alpha}_{-b}) = \frac{h_{b,l}}{I_{b,l}(\boldsymbol{\alpha}_{-b}) + \sigma_{b,l}^2}$, $l = i, k$. Therefore, $\lambda_{b,i,k}^* = 1$ if and only if $\tilde{h}_{b,i}(\boldsymbol{\alpha}_{-b}) \leq \tilde{h}_{b,k}(\boldsymbol{\alpha}_{-b})$.*

Proof. Please see Appendix A. □

Remark III.1.1. *In multi-cell NOMA, the optimal SIC ordering is the decoding order based on the ascending order of users channel gain normalized by ICI-plus-noise (called CINR-based decoding order). The optimal decoding order is independent from the power allocation policy within the cell. However, it depends on the received ICI, and subsequently on the total power consumption of neighboring (interfering) BSs.*

Corollary III.1.1. *For any given $\boldsymbol{\alpha}_{-b}$ and subsequently $\tilde{h}_{b,i}(\boldsymbol{\alpha}_{-b}) \leq \tilde{h}_{b,k}(\boldsymbol{\alpha}_{-b})$, at the optimal $\boldsymbol{\lambda}_b^*$, we have*

$$\log_2 \left(1 + \frac{p_{b,i} h_{b,i}}{\sum_{j \in \Phi_{b,i}^*} p_{b,j} h_{b,i} + (I_{b,i} + \sigma_{b,i}^2)} \right) \leq \log_2 \left(1 + \frac{p_{b,i} h_{b,k}}{\sum_{j \in \Phi_{b,i}^*} p_{b,j} h_{b,k} + (I_{b,k} + \sigma_{b,k}^2)} \right). \quad (4)$$

According to (2) and (4), at the optimal $\boldsymbol{\lambda}_b^*$, we have $R_{b,i}(\mathbf{p}, \boldsymbol{\lambda}_b^*) = \log_2 \left(1 + \frac{p_{b,i} h_{b,i}}{\sum_{j \in \Phi_{b,i}^*} p_{b,j} h_{b,i} + (I_{b,i} + \sigma_{b,i}^2)} \right)$.

According to Remark III.1.1, the centralized power allocation and SIC ordering problems cannot be decoupled. However, for given $\boldsymbol{\alpha}_{-b}$, and subsequently $\boldsymbol{\lambda}_b^*$ (based on Proposition III.1), the optimal power \mathbf{p}_b^* can be obtained in closed form according to the following proposition:

Proposition III.2. *Assume that $\boldsymbol{\alpha}_{-b}$ is fixed. For convenience, let $|\mathcal{U}_b| = M$, and $k > i$ if $\tilde{h}_{b,k}(\boldsymbol{\alpha}_{-b}) > \tilde{h}_{b,i}(\boldsymbol{\alpha}_{-b})$. According to Proposition III.1, the decoding order $M \rightarrow M-1 \rightarrow \dots \rightarrow 1$ is optimal. The optimal powers in \mathbf{p}_b^* can be obtained in closed form as follows:*

$$p_{b,i}^* = \left[\beta_{b,i} \left(\prod_{j=1}^{i-1} (1 - \beta_{b,j}) \alpha_b P_b^{max} + \frac{1}{\tilde{h}_{b,i}} - \sum_{j=1}^{i-1} \frac{\prod_{k=j+1}^{i-1} (1 - \beta_{b,k}) \beta_{b,j}}{\tilde{h}_{b,j}} \right) \right]^+, \quad \forall i = 1, \dots, M-1, \quad (5)$$

and

$$p_{b,M}^* = \left[\alpha_b P_b^{max} - \sum_{i=1}^{M-1} \beta_{b,i} \left(\prod_{j=1}^{i-1} (1 - \beta_{b,j}) \alpha_b P_b^{max} + \frac{1}{\tilde{h}_{b,i}} - \sum_{j=1}^{i-1} \frac{\prod_{k=j+1}^{i-1} (1 - \beta_{b,k}) \beta_{b,j}}{\tilde{h}_{b,j}} \right) \right]^+, \quad (6)$$

where $\beta_{b,i} = \frac{2^{R_{b,i}^{min}} - 1}{2^{R_{b,i}^{min}}}$, $\forall i = 1, \dots, M-1$, and $[.]^+ = \max\{., 0\}$.

Proof. Please see Appendix B. □

Remark III.2.1. *For sufficiently large normalized channel gains $\tilde{h}_{b,i}$, $\forall i \in \mathcal{U}_b \setminus \{M\}$, (5) and (6) can be approximated to*

$$p_{b,i}^* \approx \left[\alpha_b P_b^{max} \beta_{b,i} \left(\prod_{j=1}^{i-1} (1 - \beta_{b,j}) \right) \right]^+, \quad \forall i = 1, \dots, M-1, \quad (7)$$

and

$$p_{b,M}^* \approx \left[\alpha_b P_b^{max} \left(1 - \sum_{i=1}^{M-1} \beta_{b,i} \left(\prod_{j=1}^{i-1} (1 - \beta_{b,j}) \right) \right) \right]^+, \quad (8)$$

respectively.

Remark III.2.2. For sufficiently large normalized channel gains $\tilde{h}_{b,i}, \forall i \in \mathcal{U}_b \setminus \{M\}$, if users have the same minimum rate demands R_{\min} in cell b , the optimal power coefficient of each user $i \in \mathcal{U}_b$ denoted by $q_{b,i}^* = \frac{p_{b,i}^*}{\alpha_b P_b^{\max}}$ based on (7) and (8) can be obtained by

$$q_{b,i}^* \approx \frac{2^{R_{\min}} - 1}{(2^{R_{\min}})^i}, \quad \forall i = 1, \dots, M-1, \quad q_{b,M}^* \approx \frac{1}{(2^{R_{\min}})^{M-1}}. \quad (9)$$

Remark III.2.1 shows that in the high SINR regions, the optimal powers are approximately insensitive to the exact channel gains. Hence, (7) and (8) are valid for the fast fading and/or imperfect CSI scenarios, where the CSI variations are small such that the optimal decoding order remains constant⁹. Moreover, Remark III.2.2 shows that the weaker user always gets more power than the stronger user for the same minimum rate demands. For instance, for the case that $R_{\min} = 1$ bps/Hz, regardless of the order of NOMA cluster, near to 50% of the available power $\alpha_b P^{\max}$ will be allocated to the weakest user 1. The performance of these approximations is numerically evaluated in Subsection IV-F.

Our proposed globally optimal JSPA algorithm utilizes both the exploration of different values of α_b in $\alpha_{1 \times B}$ and the distributed power allocation optimization. In this algorithm, we perform a greedy search on different values of each α_b in $\alpha_{1 \times B}$. For given $\hat{\alpha}$, we find the optimal λ^* and p^* according to Propositions III.1 and III.2, respectively. The pseudo code of the proposed globally optimal solution is presented in Alg. 1. This algorithm needs to explore all the possible values in $\alpha_{1 \times B}$. For the total number of samples S_α for each α_b , the complexity of Alg. 1 is S_α^B . For the case that each cell has M users, the complexity of exhaustive search is $S_p^{BM} \times (M!)^B$, where S_p is the total number of samples for each $p_{b,i}$ in p . Hence, Alg. 1 reduces the complexity of exhaustive search by a factor of $S_p^M \times (M!)^B$ when $S_\alpha = S_p$. In fact, Alg. 1 has two main advantages: 1) The complexity is independent from the order of NOMA clusters resulting in low complexity method for the scenarios with larger number of users while small number of BSs; 2) The complexity of finding optimal SIC ordering is negligible since for a fixed α , the optimal decoding order is obtained in closed form.

Since the proposed Alg. 1 is still exponential in the number of BSs, it is important to check the feasibility of problem (3) with a low-complexity algorithm before performing Alg. 1. The

⁹In this work, we considered the perfect CSI scenario. The impact of imperfect CSI on the closed form of optimal powers in multi-cell NOMA can be considered as a future work.

Algorithm 1 Optimal JSPA for Sum-Rate Maximization Problem.

- 1: Initialize the step size $\epsilon_\alpha \ll 1$, and $R_{\text{tot}} = 0$.
- 2: **for** each sample $\hat{\alpha}$ **do**
- 3: Update $\tilde{h}_{b,i} = \frac{h_{b,i}}{\hat{I}_{b,i} + \sigma_{b,i}}$, $\forall b \in \mathcal{B}$, $i \in \mathcal{U}_b$, where $\hat{I}_{b,i} = \sum_{\substack{j \in \mathcal{B} \\ j \neq b}} \hat{\alpha}_j P_j^{\max} h_{j,b,i}$.
- 4: Update λ according to $\lambda_{b,i,k} = 1$ if $\tilde{h}_{b,k} > \tilde{h}_{b,i}$, or equivalently update users index according to $k > i$ if $\tilde{h}_{b,k} > \tilde{h}_{b,i}$.
- 5: Find \mathbf{p} according to (5) and (6).
- 6: **if** $\left(\sum_{b \in \mathcal{B}} \sum_{i \in \mathcal{U}_b} R_{b,i}(\mathbf{p}, \lambda_b) > R_{\text{tot}} \right)$ **then**
 Update $R_{\text{tot}}^* = \left(\sum_{b \in \mathcal{B}} \sum_{i \in \mathcal{U}_b} R_{b,i}(\mathbf{p}, \lambda_b) \right)$, $\mathbf{p}^* = \mathbf{p}$, and $\lambda^* = \lambda$.
end if
- 7: **end for**
- 8: The outputs λ^* and \mathbf{p}^* are the optimal solutions.

feasibility problem of (3) can be formulated by

$$\min_{\mathbf{p} \geq 0, \lambda \in \{0,1\}} f(\mathbf{p}, \lambda) \quad \text{s.t. (3b)-(3f)}, \quad (10)$$

where $f(\mathbf{p}, \lambda)$ can be any objective function such that the intersection of the feasible domain of (3b)-(3f) is a subset of the feasible domain of $f(\mathbf{p}, \lambda)$. Finding a feasible solution for (10) is challenging, due to the binary variables in λ . For the case that $f(\mathbf{p}) = \sum_{b \in \mathcal{B}} \sum_{i \in \mathcal{U}_b} p_{b,i}$, it is proved that the ICI (in the total power minimization problem) under the CINR-based decoding order verifies the basic properties of the standard interference function [18]. Hence, the well-known iterative distributed power minimization framework can globally solve (10) with a fast convergence speed [18]. Here, we briefly present the structure of the iterative distributed power minimization algorithm proposed in [18]. Let $\mathbf{p}^{(t-1)}$ be the output of iteration $t-1$ which is the initial power matrix for iteration t denoted by $\mathbf{p}^{(t)}$. At iteration t , we first update the optimal decoding order in cell 1 based on the updated ICI (according to Proposition III.1). Then, we find $\mathbf{p}_1^{*(t)}$ for the fixed $\mathbf{p}_{-1}^{(t)}$. After that, we substitute $\mathbf{p}_1^{(t)}$ with $\mathbf{p}_1^{*(t)}$. The updated $\mathbf{p}^{(t)}$ is an initial power matrix for the next cell 2. We repeat these steps at all the remaining cells. The updated power at cell B is the output of iteration t . We continue the iterations until the convergence is achieved. For the fixed $I_{b,i}$ and subsequently given λ_b^* in cell b , the optimal powers can be

Algorithm 2 Optimal Joint SIC Ordering and Power Allocation for Total Power Minimization Problem [18].

- 1: Initialize feasible $\mathbf{p}^{(0)}$, and tolerance ϵ_{tol} (sufficiently small).
- 2: **while** $\|\mathbf{p}^{(t-1)}\| - \|\mathbf{p}^{(t)}\| > \epsilon_{\text{tol}}$ **do**
- 3: Set $t =: t + 1$, and then update $\mathbf{p}^{(t)} =: \mathbf{p}^{(t-1)}$.
- 4: **for** $b=1:B$ **do**
- 5: Update the ICI term $I_{b,i} = \sum_{\substack{j \in \mathcal{B} \\ j \neq b}} \left(\sum_{l \in \mathcal{U}_j} p_{j,l} \right) h_{j,b,i}$ at cell b .
- 6: Update $\boldsymbol{\lambda}_b$ in cell b according to $k \rightarrow i$ if $\tilde{h}_{b,k} > \tilde{h}_{b,i}$, where $\tilde{h}_{b,l} = \frac{h_{b,l}}{I_{b,l} + \sigma_{b,l}}$, $\forall b \in \mathcal{B}$, $l \in \mathcal{U}_b$.
- 7: Find $\mathbf{p}_b^{*(t)}$ using (11). Then, substitute $\mathbf{p}_b^{(t)}$ with $\mathbf{p}_b^{*(t)}$.
- 8: **end for**
- 9: **end while**
- 10: The outputs $\boldsymbol{\lambda}^*$ and \mathbf{p}^* are the optimal solutions.

obtained in closed form as

$$p_{b,i}^* = \beta_{b,i} \left(\prod_{j=i+1}^M (1 + \beta_{b,j}) + \frac{1}{\tilde{h}_{b,i}} + \sum_{j=i+1}^M \frac{\beta_{b,j} \prod_{k=i+1}^{j-1} (1 + \beta_{b,k})}{\tilde{h}_{b,j}} \right), \quad \forall i = 1, \dots, M. \quad (11)$$

where $\beta_{b,i} = 2^{R_{b,i}^{\min}} - 1$, $\forall i = 1, \dots, M$ and $\tilde{h}_{b,l} = \frac{h_{b,l}}{I_{b,l} + \sigma_{b,l}}$. For convenience, in (11), we assumed that $|\mathcal{U}_b| = M$ and also updated the users index based on the ascending order of $\tilde{h}_{b,i}$. For more details, please see Appendix C. The pseudo code of the proposed power minimization algorithm is presented in Alg. 2. Numerical assessments show that Alg. 2 has a very fast convergence speed [18]. The only concern is finding a feasible initial point $\mathbf{p}^{(0)}$. In Subsection IV-D, we provided comprehensive discussions about the impact of feasible/infeasible initial points on the convergence of Alg. 2.

It is proved that the optimal $\boldsymbol{\alpha}^*$ in the total power minimization problem is indeed a component-wise minimum [18]. It means that for any feasible $\hat{\boldsymbol{\alpha}} = [\hat{\alpha}_b], \forall b \in \mathcal{B}$ in (10), it can be guaranteed that $\alpha_b^* \leq \hat{\alpha}_b$. As a result, the exploration area of each α_b in Alg. 1 can be reduced from $[0, 1]$ to $[\alpha_b^{\min}, 1]$, where α_b^{\min} denotes the optimal power consumption coefficient of BS b in the total power minimization problem. The lower-bounds $\alpha_b^{\min}, \forall b \in \mathcal{B}$ can significantly reduce the complexity of Alg. 1 for the case that α_b^{\min} grows, e.g., when the minimum rate demand of users increases.

2) *Suboptimal SIC Ordering: Joint Rate and Power Allocation:* According to Proposition III.1, since λ^* in (3) depends on α_{-b}^* , any decoding order before power allocation is indeed suboptimal. For any suboptimal decoding order, Corollary III.1.1 may not hold and thus, NOMA is not capacity-achieving. The main problem (3) for given λ , or equivalently fixed $\Phi_{b,i}$, can be rewritten as

$$\max_{\mathbf{p} \geq 0} \sum_{b \in \mathcal{B}} \sum_{i \in \mathcal{U}_b} R_{b,i}(\mathbf{p}) \quad \text{s.t. (3b), (3c).} \quad (12)$$

Constraint (3c) can be equivalently transformed to a linear form as follows:

$$2^{R_{b,i}^{\min}} \left(\sum_{j \in \Phi_{b,i}} p_{b,j} h_{b,k} + I_{b,k} + \sigma_{b,k}^2 \right) \leq \left(p_{b,i} + \sum_{j \in \Phi_{b,i}} p_{b,j} \right) h_{b,k} + I_{b,k} + \sigma_{b,k}^2, \quad \forall b \in \mathcal{B},$$

$$i, k \in \mathcal{U}_b, \quad k \in \{i\} \cup \Phi_{b,i}. \quad (13)$$

Hence, the feasible region of (12) is affine, so is convex in \mathbf{p} . However, (12) is still strongly NP-hard, due to the nonconcavity of the sum-rate function with respect to \mathbf{p} . The optimal powers in (5) and (6) are derived based on the optimal decoding order. Hence, Alg. 1 is not applicable for solving (12). Besides, the complexity of exhaustive search for solving (12) is S_p^{BM} , which is exponential in the number of users. In the following, we apply the sequential programming approach [29] to find a suboptimal power allocation for (12). To tackle the non-differentiability of $R_{b,i}(\mathbf{p})$, we first apply the epigraph technique [15], and define $r_{b,i}$ as the adopted spectral efficiency of user $i \in \mathcal{U}_b$ such that $r_{b,i} \leq \log_2 \left(1 + \frac{p_{b,i} h_{b,k}}{\sum_{j \in \Phi_{b,i}} p_{b,j} h_{b,k} + I_{b,k} + \sigma_{b,k}^2} \right)$, $\forall b \in \mathcal{B}$, $i, k \in \mathcal{U}_b$, $k \in \{i\} \cup \Phi_{b,i}$. Hence, (12) can be equivalently transformed to the following problem as

$$\text{JRPA : } \max_{\mathbf{p} \geq 0, \mathbf{r} \geq 0} \sum_{b \in \mathcal{B}} \sum_{i \in \mathcal{U}_b} r_{b,i} \quad (14a)$$

s.t. (3b),

$$r_{b,i} \geq R_{b,i}^{\min}, \quad \forall b \in \mathcal{B}, \quad i \in \mathcal{U}_b, \quad (14b)$$

$$r_{b,i} \leq \log_2 \left(1 + \frac{p_{b,i} h_{b,k}}{\sum_{j \in \Phi_{b,i}} p_{b,j} h_{b,k} + I_{b,k} + \sigma_{b,k}^2} \right), \quad \forall b \in \mathcal{B}, \quad i, k \in \mathcal{U}_b, \quad k \in \{i\} \cup \Phi_{b,i},$$

$$(14c)$$

where $\mathbf{r} = [r_{b,i}]$, $\forall b \in \mathcal{B}, i \in \mathcal{U}_b$. Although the objective function (14a) and constraints (3b) and (14b) are affine, problem (14) is still nonconvex due to the nonconvexity of (14c). The derivations

Algorithm 3 Suboptimal JRPA Algorithm Based on the Sequential Programming.

- 1: Initialize $\mathbf{r}^{(0)}$, iteration index $t = 0$, and tolerance $\epsilon_s \ll 1$.
- 2: **while** $\|\mathbf{r}^{(t)} - \mathbf{r}^{(t-1)}\| > \epsilon_s$ **do**
- 3: Set $t =: t + 1$.
- 4: Update the approximation parameter $\hat{g}(r_{b,i}^{(t)})$ based on $\mathbf{r}^{*(t-1)}$.
- 5: Find $(\mathbf{r}^{*(t)}, \tilde{\mathbf{p}}^{*(t)})$ by solving the convex approximated problem (40).
- 6: **end while**
- 7: Set $p_{b,i}^* = e^{\tilde{p}_{b,i}^*}$, $\forall b \in \mathcal{B}$, $i \in \mathcal{U}_b$. The outputs $(\mathbf{r}^{*(t)}, \mathbf{p}^{*(t)})$ are adopted for the network.

of the proposed sequential programming method for solving (14) is presented in Appendix D. The pseudo code of our proposed JRPA algorithm is shown in Alg. 3.

The decoding order for some user pairs is independent from the ICI, so it can be determined prior to power allocation optimization. For a specific channel gain condition, we prove that the CNR-based decoding order is optimal for a user pair independent from power allocation.

Theorem 1. (SIC sufficient condition) For each user pair $i, k \in \mathcal{U}_b$ with $\frac{h_{b,k}}{\sigma_{b,k}} \geq \frac{h_{b,i}}{\sigma_{b,i}}$, if

$$\frac{h_{b,k}}{\sigma_{b,k}} - \frac{h_{b,i}}{\sigma_{b,i}} \geq \sum_{j \in \mathcal{Q}_{b,i,k}} \frac{P_j^{\max}}{\sigma_{b,i}\sigma_{b,k}} (h_{j,b,k}h_{b,i} - h_{j,b,i}h_{b,k}), \quad (15)$$

where $\mathcal{Q}_{b,i,k} = \left\{ j \in \mathcal{B} \setminus \{b\} \mid \frac{h_{b,k}}{h_{b,i}} < \frac{h_{j,b,k}}{h_{j,b,i}} \right\}$, the decoding order $k \rightarrow i$ is optimal.

Proof. Please see Appendix E. □

Theorem 1 shows that the optimal decoding order is challenging for only the user pairs in which their ICIs affect the sign of their CINR difference. Assume that the suboptimal CNR-based decoding order is applied in (14), i.e., $k \rightarrow i$ or $\lambda_{b,i,k} = 1$ if $\frac{h_{b,k}}{\sigma_{b,k}} \geq \frac{h_{b,i}}{\sigma_{b,i}}$. Let us define the set of users with higher decoding orders than user $i \in \mathcal{U}_b$ that satisfy the SIC sufficient condition by $\Phi_{b,i}^{\text{CNR}} = \{k \in \mathcal{U}_b \setminus \{i\} \mid \lambda_{b,i,k} = 1, \frac{h_{b,k}}{\sigma_{b,k}} - \frac{h_{b,i}}{\sigma_{b,i}} \geq \sum_{j \in \mathcal{Q}_{b,i,k}} \frac{P_j^{\max}}{\sigma_{b,i}\sigma_{b,k}} (h_{j,b,k}h_{b,i} - h_{j,b,i}h_{b,k})\}$.

Obviously, we have $\Phi_{b,i}^{\text{CNR}} \subseteq \Phi_{b,i}$. Based on Theorem 1, it is required to check the feasibility of constraint (14c) for only users in $\{i\} \cup \Phi_{b,i} \setminus \Phi_{b,i}^{\text{CNR}}$, which significantly reduces the complexity of our proposed JRPA algorithm. For the case that $\Phi_{b,i}^{\text{CNR}} = \Phi_{b,i}$, we can guarantee that Corollary (III.1.1) holds for user $i \in \mathcal{U}_b$, meaning that $r_{b,i}^* = \tilde{R}_{b,i}(\mathbf{p}^*, \boldsymbol{\lambda}_b^*)$. Finally, for the case that the SIC sufficient condition holds for every user pair within cell b , i.e., $\Phi_{b,i}^{\text{CNR}} = \Phi_{b,i}$, $\forall i \in \mathcal{U}_b$, the

CNR-based decoding order is optimal in cell b , meaning that the number of constraints in (14c) will be reduced to one in that cell.

Similar to problem (10), it can be shown that the feasible region of (12) is the same as the feasible region of the following total power minimization problem as

$$\min_{\mathbf{p} \geq 0, \mathbf{r} \geq 0} \sum_{b \in \mathcal{B}} \sum_{i \in \mathcal{U}_b} p_{b,i} \quad \text{s.t. (3b), (13).} \quad (16)$$

Since the objective function and all the constraints are affine, problem (16) is a linear program, so is convex. Hence, (16) can be solved by using the Dantzig's simplex method or interior-point methods (IPMs) [15]. The solution of (16) can be utilized as initial feasible point for Alg. 3.

3) *Suboptimal SIC Ordering: Power Allocation for a Fixed Rate Region:* In Subsection III-A2, we showed that for any suboptimal decoding order (fixed λ), Corollary III.1.1 may not hold, so joint power allocation and rate adoption is necessary to achieve the maximum possible spectral efficiency of the users. There are a number of research studies in multi-cell NOMA assuming a fixed rate region for each user as $\hat{R}_{b,i} = \log_2 \left(1 + \frac{p_{b,i}h_{b,i}}{\sum_{j \in \Phi_{b,i}} p_{b,j}h_{b,i} + (I_{b,i}(\mathbf{p}_{-b}) + \sigma_{b,i}^2)} \right)$ eliminating the exploration area of finding optimal rate allocation [20], [23], [25]–[27]. According to (2), to guarantee that user $i \in \mathcal{U}_b$ achieves its Shannon's capacity for decoding its desired signal after successful SIC at users, the condition in (4) should be satisfied for each user $k \in \Phi_{b,i}$. For a fixed λ , so fixed $\Phi_{b,i}$, (4) can be rewritten as

$$\frac{h_{b,i}}{I_{b,i} + \sigma_{b,i}^2} \leq \frac{h_{b,k}}{I_{b,k} + \sigma_{b,k}^2}, \quad \forall b \in \mathcal{B}, i, k \in \mathcal{U}_b, k \in \Phi_{b,i}. \quad (17)$$

The constraint in (17) is known as SIC necessary condition [20], [23], [25].

Fact III.2.1. *In multi-cell NOMA, the SIC necessary condition (17) for each user pair $i, k \in \mathcal{U}_b$, $k \in \Phi_{b,i}$ implies additional maximum power constraints on the BSs in $\mathcal{B} \setminus \{b\}$.*

Proof. Please see Appendix F. □

Remark III.2.3. *Restricting the rate region of users under the suboptimal decoding order results in additional limitations on the BSs power consumption. For the user pairs satisfying the SIC sufficient condition, the decoding order is optimal, and subsequently the SIC constraint (17) will be completely independent from the power allocation (see Corollary III.1.1). As a result, the negative side impact of the SIC necessary condition in power allocation will be eliminated.*

According to (3), for any fixed λ , the power allocation problem for the suboptimal decoding order and fixed rate region, called fixed-rate-region power allocation (FRPA), is formulated by

$$\text{FRPA} : \max_{\mathbf{p} \geq 0} \sum_{b \in \mathcal{B}} \sum_{i \in \mathcal{U}_b} \tilde{R}_{b,i}(\mathbf{p}) \quad (18a)$$

$$\text{s.t. (3b), (17),} \quad (18b)$$

$$\tilde{R}_{b,i}(\mathbf{p}) \geq R_{b,i}^{\min}, \quad \forall b \in \mathcal{B}, \quad i \in \mathcal{U}_b. \quad (18c)$$

Constraints (18c) and (17) can be equivalently transformed to linear forms in \mathbf{p} as (13) and (41), respectively. Therefore, the feasible region of (18) is affine, so is convex. However, the sum-rate function in (18a) is nonconcave, due to the existing ICI, which makes the main problem (18) nonconvex and strongly NP-hard [23], [25]. Problem (18) can be solved by using the monotonic optimization proposed in [29]. However, the complexity of monotonic optimization is still exponential in the number of users [29]. According to Corollary III.1.1, under the optimal decoding order λ^* , the main problem (3) can be rewritten as

$$\max_{\mathbf{p} \geq 0} \sum_{b \in \mathcal{B}} \sum_{i \in \mathcal{U}_b} \tilde{R}_{b,i}(\mathbf{p}) \quad (19a)$$

$$\text{s.t. (3b),} \quad (19b)$$

$$\tilde{R}_{b,i}(\mathbf{p}) \geq R_{b,i}^{\min}, \quad \forall b \in \mathcal{B}, \quad i \in \mathcal{U}_b. \quad (19c)$$

The feasible region of (19) and (18) is the same for the case that the SIC necessary condition (17) is removed from (18). According to Fact III.2.1, the constraint (17) adds additional restriction on the feasible region of (18). As a result, the feasible region of (18) is a subset of the feasible region of (19). In this regard, the optimal solution of (18) lies on the intersection of the feasible region of (19) and constraint (17). Accordingly, Alg. 1 can be modified based on the fixed λ and SIC constraint (17) to find the globally optimal solution of (18). The pseudo code of the globally optimal solution for (18) is presented in Alg. 4. The main difference of Algs. 1 and 4 is Step 4. In Alg. 4, we check the SIC necessary condition for the fixed decoding order instead of updating the SIC decoding orders in Alg. 1. Although Alg. 4 scales well with any number of multiplexed users, it is still exponential in the number of BSs (see Subsection III-A1). One solution is to apply the well-known suboptimal power allocation based on the sequential programming method proposed in [23], [25], [29].

Algorithm 4 Optimal Power Allocation for Fixed SIC Ordering and Rate Region.

- 1: Initialize the step size $\epsilon_\alpha = \frac{1}{S_\alpha} \ll 1$, where S_α is the number of samples for each α_b , and $R_{\text{tot}} = 0$.
- 2: **for** each sample $\hat{\alpha}$ **do**
- 3: Update $\tilde{h}_{b,i} = \frac{h_{b,i}}{\hat{I}_{b,i} + \sigma_{b,i}^2}$, $\forall b \in \mathcal{B}$, $i \in \mathcal{U}_b$, where $\hat{I}_{b,i} = \sum_{\substack{j \in \mathcal{B} \\ j \neq b}} \hat{\alpha}_j P_j^{\max} h_{j,b,i}$.
- 4: **if** $\left(\frac{h_{b,i}}{I_{b,i} + \sigma_{b,i}^2} \leq \frac{h_{b,k}}{I_{b,k} + \sigma_{b,k}^2}, \forall b \in \mathcal{B}, i, k \in \mathcal{U}_b, k \in \Phi_{b,i} \right)$ **then**
- 5: Find \mathbf{p} according to (5) and (6).
- 6: **if** $\left(\sum_{b \in \mathcal{B}} \sum_{i \in \mathcal{U}_b} R_{b,i}(\mathbf{p}) > R_{\text{tot}} \right)$ **then**
- 7: Update $R_{\text{tot}}^* = \left(\sum_{b \in \mathcal{B}} \sum_{i \in \mathcal{U}_b} R_{b,i}(\mathbf{p}) \right)$, and $\mathbf{p}^* = \mathbf{p}$.
- 8: **end if**
- 9: **end if**
- 10: **end for**
- 11: The output \mathbf{p}^* is the optimal solution of (18).

The feasible solution for (18) can be obtained by solving the following total power minimization problem as

$$\min_{\mathbf{p} \geq 0} \sum_{b \in \mathcal{B}} \sum_{i \in \mathcal{U}_b} p_{b,i} \quad \text{s.t. (3b), (17), (18c).} \quad (20)$$

Problem (20) is a linear program which can be solved by using the Dantzig's simplex method.

B. Decentralized Resource Management Frameworks

1) *Fully Distributed JSPA Framework*: Although the globally optimal solution in Subsection III-A1 achieves the channel capacity of users, the complexity of Alg. 1 is still exponential in the number of BSs. Moreover, the centralized framework would cause a large signaling overhead. Here, we propose a fully distributed resource allocation framework in which each BS independently allocates power to its associated users. Actually, we divide the main problem (3) into B single-cell NOMA problems.

Fact III.2.2. *At the optimal point of sum-rate maximization problem of single-cell NOMA, the BS operates in its maximum available power. It means that the power constraint (3b) is active for each BS b , i.e., $\sum_{i \in \mathcal{U}_b} p_{b,i}^* = P_b^{\max}$, $\forall b \in \mathcal{B}$ in the fully distributed framework.*

Proof. Please see Appendix G. □

According to Fact III.2.2, we set $\alpha_b^* = 1$, $\forall b \in \mathcal{B}$. Based on the given α^* , the optimal decoding order of users under the fully distributed framework can be easily obtained by Proposition III.1. According to Subsection III-A1, the optimal power p^* under the fully distributed framework can be obtained by using Proposition III.2.

2) *Semi-Centralized JSPA Framework:* The fully distributed framework works well for the case that the ICI levels are significantly low, so $\alpha_b^* \rightarrow 1$, $\forall b \in \mathcal{B}$ in problem (3). For the case that the ICI levels are high, e.g., at femto-cells underlying a single MBS [28], the fully distributed framework may seriously degrade the spectral efficiency of femto-cell users. In the following, we propose a semi-centralized JSPA framework in which we assume that the low-power FBSs operate in their maximum power, while the MBS power consumption is obtained by the joint power allocation and SIC ordering of all the users. Let $b = 1$ be the MBS's index, and $b = 2, \dots, B$ be the index of FBSs. In this framework, we assume that $\alpha_b = 1$, $\forall b = 2, \dots, B$. Then, we utilize Alg. 1 to find the globally optimal p^* and λ^* for problem (3). This algorithm performs a grid search on $0 \leq \alpha_1 \leq 1$. Hence, the complexity of finding optimal JSPA is on the order of total number of samples for α_1 , i.e., S_α . Actually, the computational complexity of this algorithm is independent from the number of FBSs and users which is a good solution for the large-scale systems. The performance of the semi-centralized framework depends on the FBSs optimal power consumption in (3). For the case that $\alpha_b^* \rightarrow 1$, $\forall b = 2, \dots, B$ in (3), the performance gap between the semi-centralized and centralized frameworks tends to zero.

C. Computational Complexity Comparison Between Resource Allocation Algorithms

In this section, we compare the computational complexity of the proposed different resource allocation algorithms for solving the sum-rate maximization problem (3). To simplify the analysis, we assume that each cell has M users. In this comparison, we apply the barrier method with inner Newton's method to achieve an ϵ -suboptimal solution for a convex problem. The number of barrier iterations required to achieve $\frac{m}{t} = \epsilon$ -suboptimal solution is exactly $\Upsilon = \lceil \frac{\log(m/(\epsilon t^{(0)}))}{\log \mu} \rceil$, where m is the total number of inequality constraints, $t^{(0)}$ is the initial accuracy parameter for approximating the functions in inequality constraints in standard form, and μ is the step size for updating the accuracy parameter t [15]. The number of inner Newton's iterations at each barrier iteration i is denoted by N_i . In general, N_i depends on μ and how good is the initial

points at the barrier iteration i . The computational complexity of solving a convex problem is thus on the order of total number of Newton's iterations obtained by $C_{\text{cnvx}} = \sum_{i=1}^{\Upsilon} N_i$. For the case that the sequential programming converges in Q iterations, the complexity of this method is on the order of $C_{\text{SP}} = \sum_{q=1}^Q \sum_{i=1}^{\Upsilon} N_{q,i}$, where $N_{q,i}$ denotes the number of inner Newton's iterations at the i -th barrier iteration of the q -th sequential iteration. For convenience, assume that $N_{q,i} = N$, $\forall q = 1, \dots, Q$, $i = 1, \dots, \Upsilon$. Hence, we have $C_{\text{cnvx}} = N\Upsilon = N \lceil \frac{\log(m/(\epsilon t^{(0)}))}{\log \mu} \rceil$, and $C_{\text{SP}} = QN\Upsilon = QN \lceil \frac{\log(m/(\epsilon t^{(0)}))}{\log \mu} \rceil$. The complexity order of different solution algorithms for (3) is presented in Table I. In this table, S denotes the number of samples for each $p_{b,i}$ or

TABLE I
COMPUTATIONAL COMPLEXITY OF RESOURCE ALLOCATION ALGORITHMS FOR SOLVING THE SUM-RATE MAXIMIZATION PROBLEM.

Algorithm	Complexity	Framework	Optimal	λ	r	α	p
JSPA (Alg. 1)	S^B	Centralized	✓	✓	✓	✓	✓
Exhaustive Search	$(M!)^B \times S^{BM}$	Centralized	✓	✓	✓	✓	✓
JRPA (Alg. 3)	$QN \lceil \frac{\log((B+BM+B(\frac{M-1}{2}))/(\epsilon t^{(0)}))}{\log \mu} \rceil$	Centralized	✗	✗	✓	✓	✓
FRPA	S^B	Centralized	✓	✗	✗	✓	✓
Monotonic Optimization [23], [29]	$\approx S^{BM}$	Centralized	✓	✗	✗	✓	✓
Sequential Program [23], [29]	$QN \lceil \frac{\log((B+BM+B(\frac{M-1}{2}))/(\epsilon t^{(0)}))}{\log \mu} \rceil$	Centralized	✗	✗	✗	✓	✓
Subsection III-B2	S	Semi-Centralized	✓	✓	✓	α_1	✓
Subsection III-B1	1	Fully Distributed	✓	✓	✓	✗	✓

α_b . Moreover, the optimality status is for only the simplified problem. For example, FRPA finds the globally optimal powers in p , and subsequently α , when λ and r are fixed. It does not mean that the output is globally optimal solution for the main problem (3). Actually, only the first and second rows in Table I can find the globally optimal solution of (3), and the rest of the algorithms are indeed suboptimal. It is noteworthy that in Table I, we considered the highest possible computational complexity (worst case) of each algorithm.

IV. NUMERICAL RESULTS

In this section, we evaluate the performance of our proposed resource allocation algorithms via MATLAB Monte Carlo simulations through 10000 network realizations [18]. This comparison is divided into two subsections: 1) performance comparison among our proposed JSPA, JRPA, and FRPA algorithms to demonstrate the benefits of optimal SIC ordering, and rate adoption

TABLE II
SYSTEM PARAMETERS

Parameter	Notation	Value	Parameter	Notation	Value
Coverage of MBS	\times	500 m	Lognormal shadowing standard deviation	\times	8 dB
Coverage of FBS	\times	40 m	Small-scale fading	\times	Rayleigh fading
Distance between MBS and FBS	\times	200 m	AWGN power density	$N_{b,i}$	-174 dBm/Hz
Number of macro-cell users	$ \mathcal{U}_m $	{2;3;4}	MBS transmit power	P_m^{\max}	46 dBm
Number of femto-cell users	$ \mathcal{U}_f $	{2;3;4;5;6}	FBS transmit power	P_f^{\max}	30 dBm
User distribution model	\times	Uniform	Minimum rate of macro-cell users	R_m^{\min}	{0.5; 1; 2} bps/Hz
Minimum distance of users to MBS	\times	20 m	Minimum rate of femto-cell users	R_f^{\min}	{0.25; 0.50; 0.75; 1; 2; 3} bps/Hz
Minimum distance of users to FBS	\times	2 m	Tolerance of Alg. 2	ϵ_{tol}	10^{-6}
Wireless bandwidth	\times	5 MHz	Step size of each $\alpha_b \in [0, 1]$	ϵ_{α}	10^{-2}
MBS path loss	\times	$128.1 + 37.6 \log_{10}(d/\text{Km})$ dB	Tolerance of Alg. 3	ϵ_s	10^{-1}
FBS path loss	\times	$140.7 + 36.7 \log_{10}(d/\text{Km})$ dB	-	-	-

for any suboptimal decoding order (see Table I); 2) performance comparison among the centralized and decentralized resource allocation frameworks to demonstrate the effect of optimal α^* (ICI management) in the main problem (3). In our simulations, we adopt the commonly-used (suboptimal) CNR-based decoding order [23], [25] for the JRPA and FRPA algorithms. Finally, we evaluate the convergence of the iterative algorithms for solving (10) and (14), and the performance of approximated optimal powers in Remark III.2.1. The complete source code is available on GitLab [30].

A. Simulation Settings

Here, we consider a two-tier HetNet consisting of one FBS underlying a MBS¹⁰. Within each cell, there is one BS at the center of a circular area and \mathcal{U}_b users inside it [18]. The system parameters and their corresponding notations are shown in Table II. The network topology and exemplary users placement are shown in Fig. 1.

B. Performance of Centralized Resource Allocation Algorithms

In this subsection, we compare the performance in terms of outage probability, and users total spectral efficiency of our proposed JSPA, JRPA, and FRPA algorithms. Note that FRPA finds the globally optimal solution of the sum-rate maximization problem in [25] and the single-carrier-based downlink power allocation problem in [23] with significantly reduced computational complexity (see Table I).

¹⁰Although in practice there are larger number of FBSs, in this experiment, we aim to fundamentally investigate the impact of ICI from MBS to FBS and vice versa in optimal decoding order of users.

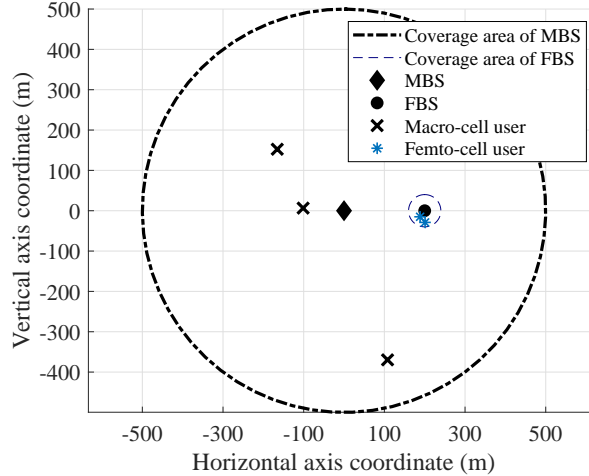
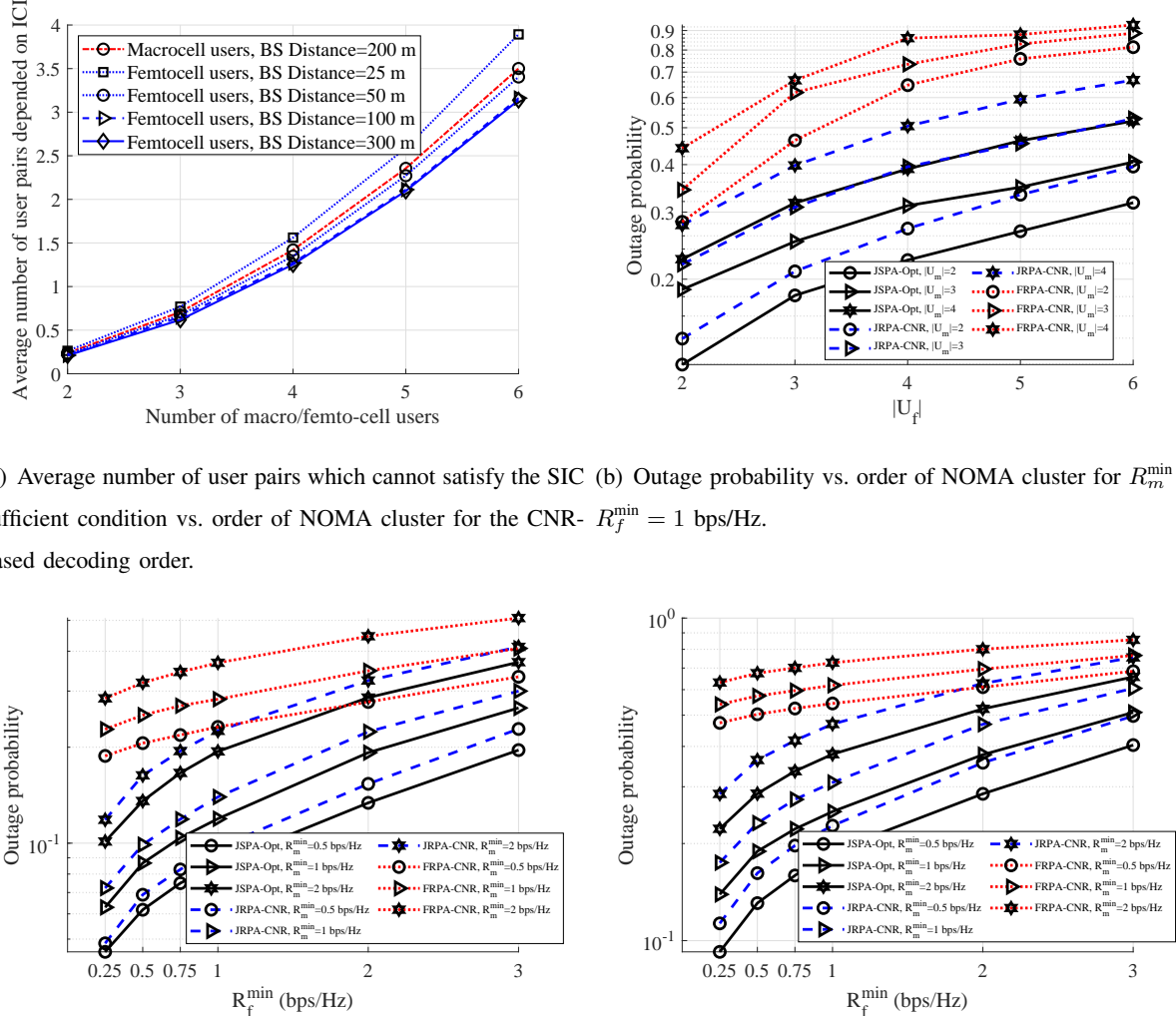


Fig. 1. Network topology and exemplary user placement for $|\mathcal{U}_m| = 3$, and $|\mathcal{U}_f| = 2$.

1) *Outage Probability Performance*: The outage probability of the JSPA, JRPA, and FRPA schemes is obtained based on optimally solving their corresponding total power minimization problems (10), (16), and (20), respectively. For each scheme, the outage probability is calculated by dividing the number of infeasible problem instances by total number of samples [18]. Fig. 2 shows the impact of order of NOMA clusters and minimum rate demands on the outage probability of the JSPA, JRPA, and FRPA problems. According to Theorem 1, the ICI may affect the optimal decoding order of user pairs which cannot satisfy the SIC sufficient condition. We call these user pairs as the pairs depending on ICI when the CNR-based decoding order is applied. In Fig. 2(a), we calculate the average number of user pairs depending on ICI (denoted by Ψ) for different distances among BSs, and different order of NOMA clusters in the CNR-based decoding order. The parameter Ψ is increased by 1) increasing $|\mathcal{U}_b|$, which inherently decreases the LHS of (15); 2) increasing the inter-cell channel gain $h_{j,b,i}$, due to increasing the RHS of (15). The second case for the femto-cell user pairs is inversely proportional to the BSs distance, due to the existing path loss. As shown, the impact of $|\mathcal{U}_b|$ is higher than the impact of BSs distance. The wide coverage of macro-cell results in large differences between the users channel gains, however the CNR of macro-cell users is typically low reducing the LHS of (15). As a result, Ψ is also affected by $|\mathcal{U}_m|$. It is noteworthy that the position of FBS (BSs distance) in the coverage area of MBS does not have significant impact on Ψ for the macro-cell users. For the case that at least one user pair within a cell does not satisfy the SIC sufficient condition,



(c) Outage probability vs. users minimum rate demand for 2-order NOMA clusters. (d) Outage probability vs. users minimum rate demand for 3-order NOMA clusters.

Fig. 2. Outage probability of the centralized JSPA, JRPA, and FRPA algorithms for different number of users and minimum rate demands.

the CNR-based decoding order in that cell may not be optimal, resulting in reduced spectral efficiency and increased outage.

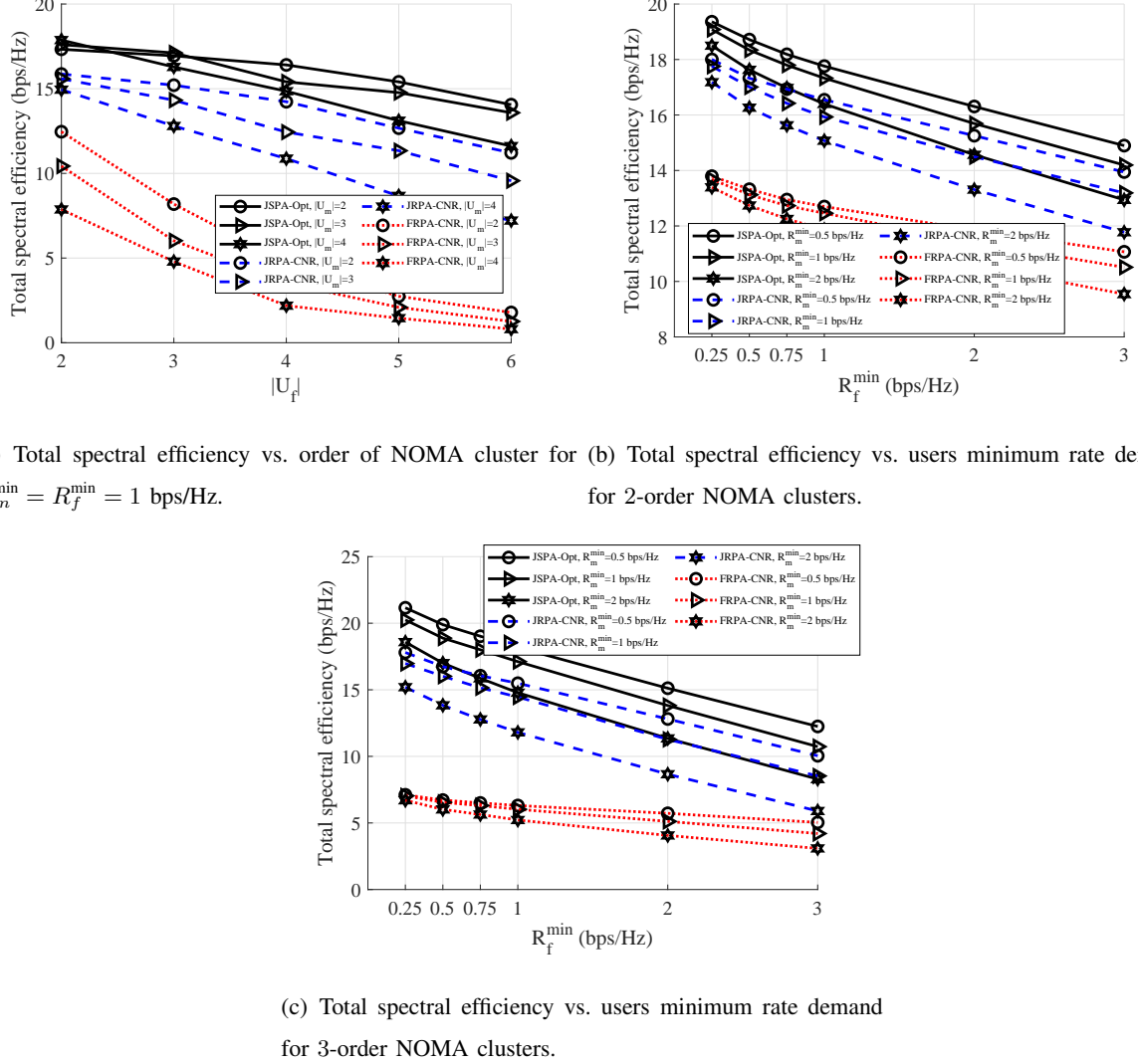
In Figs. 2(b)-2(d), we observe that there exist significant performance gaps between the JSPA and JRPA schemes, which shows the superiority of finding the optimal decoding order in multi-cell NOMA. Besides, JRPA significantly reduces the outage probability of the FRPA scheme which shows the importance of rate adoption when a suboptimal decoding order is applied. The large performance gap between JSPA and FRPA shows that the SIC necessary condition in (17) seriously restricts the feasible region of the FRPA problem (see Fact III.2.1) resulting in high

outage, specifically for the larger order of NOMA clusters (see Fig. 2(b)). Last but not least, in Fig. 2(b), we observe that a larger order of NOMA clusters results in high outage probability even for the optimal JSPA algorithm. Therefore, it is not wise to multiplex all the users when considering a large number of users within a cell. The common solution is to divide the users into multiple groups in which each user group operates in an isolated subband [18], [20], [25]. From the practical implementation, another disadvantages of increasing the order of NOMA clusters are increasing the receivers complexity and error propagation due to SIC [5], [18]. Finding the optimal JSPA for maximizing users sum-rate in the general multi-carrier multi-cell NOMA system can be considered as a future work.

2) *Total Spectral Efficiency Performance*: Fig. 3 investigates the impact of order of NOMA clusters and minimum rate demands on the average total spectral efficiency of users. Here, we set the sum-rate to zero when the problem is infeasible. As shown, JSPA always outperforms the JRPA and FRPA algorithms. The resulting performance gap between JSPA and JRPA is indeed an upper-bound of the exact performance gap between the optimal and CNR-based decoding orders, since Alg. 3 provides a lower-bound for the optimal value of (14) (see Table I). In Subsection IV-E, we show that JRPA is a near to optimal algorithm, so this lower-bound is significantly tighten. Subsequently, the performance gap between JRPA and FRPA is indeed the lower-bound of the exact performance gain of rate adoption for the CNR-based decoding order. As can be seen, FRPA has a significantly lower performance compared to JRPA. In Fig. 3(a), we observe that for $R_m^{\min} = R_f^{\min} = 1$ bps/Hz, the negative side impact of increasing the order of NOMA cluster is higher than the multi-user diversity gain. As a result, increasing the order of NOMA clusters results in lower total spectral efficiency. Another reason is increasing the outage probability (shown in Fig. 2(b)) which can significantly affect the average total spectral efficiency. For $|\mathcal{U}_m| = |\mathcal{U}_f| = 2$, we observed that the performance gap is low between JSPA and JRPA, due to decreasing Ψ in Fig. 2(a). This performance gap grows when $|\mathcal{U}_b|$ increases. As is expected, Figs. 3(b) and 3(c) show that the total spectral efficiency of users is decreasing in minimum rate demands. More importantly, there exist huge performance gaps between JSPA and FRPA for any number of users and minimum rate demands.

C. Performance of Centralized and Decentralized Frameworks

In this subsection, we compare the performance of the centralized, semi-centralized, and fully distributed JSPA frameworks (shown in Table I).



(a) Total spectral efficiency vs. order of NOMA cluster for 2-order NOMA clusters.
(b) Total spectral efficiency vs. users minimum rate demand $R_m^{\min} = R_f^{\min} = 1$ bps/Hz.
for 2-order NOMA clusters.

Fig. 3. Total spectral efficiency of the centralized JSPA, JRPA, and FRPA algorithms for different number of users and minimum rate demands.

1) *Outage Probability Performance*: Fig. 4 evaluates the outage probability of different resource allocation frameworks. As can be seen, the fully distributed framework results in huge outage probability. However, the outage probability gap between the semi-centralized and centralized frameworks is decreasing with larger $|\mathcal{U}_m|$ (Fig. 4(a)), and/or higher R_m^{\min} (Figs. 4(b) and 4(c)). The large performance gap between the semi-centralized and fully distributed frameworks shows the importance of ICI management from MBS to femto-cell users. It is noteworthy that the feasible point for the semi-centralized framework is obtained based on the gread search on α_1 with stepsize $\epsilon_\alpha = 10^{-2}$. Although it can be shown that further reducing ϵ_α would not cause

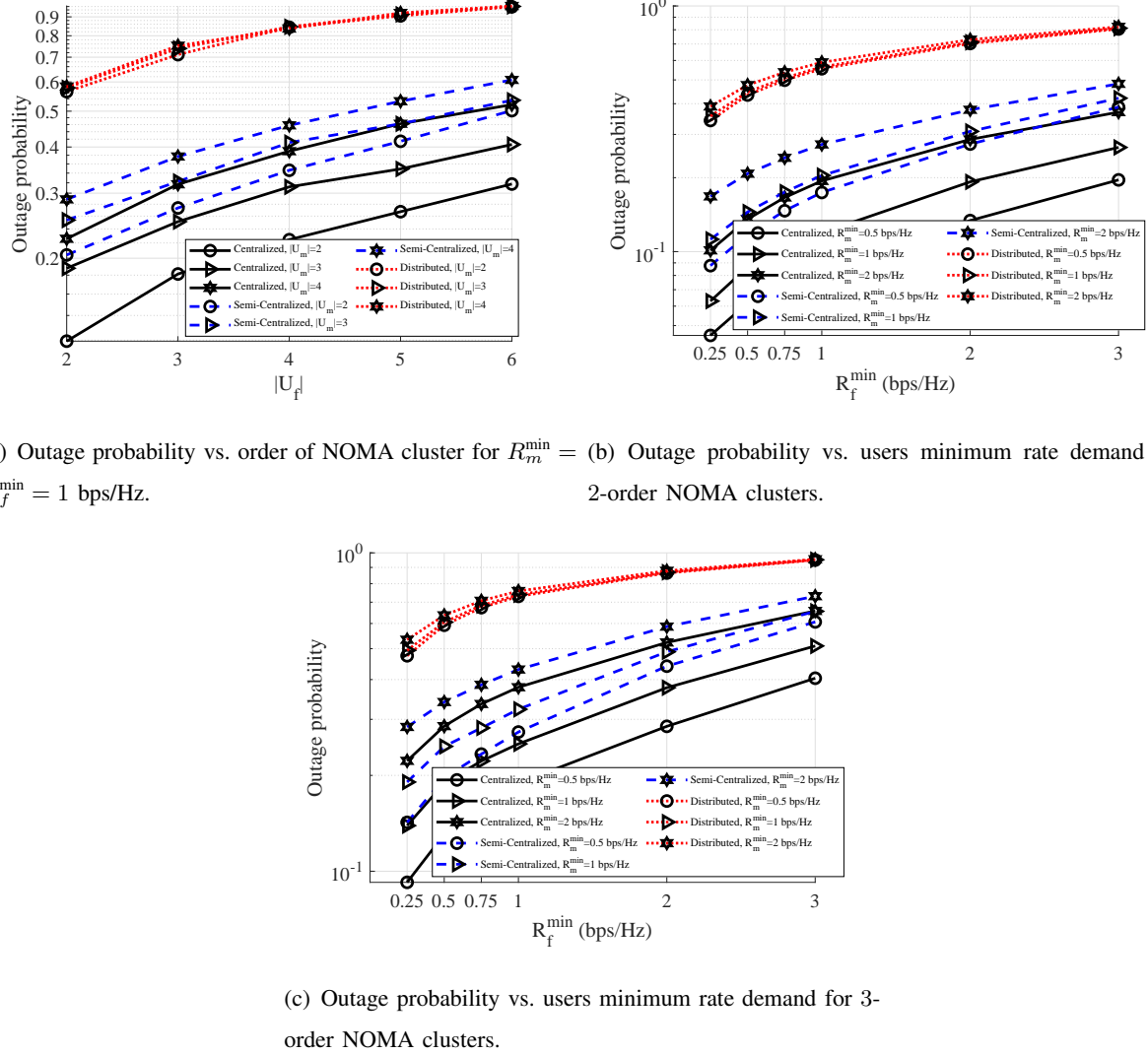
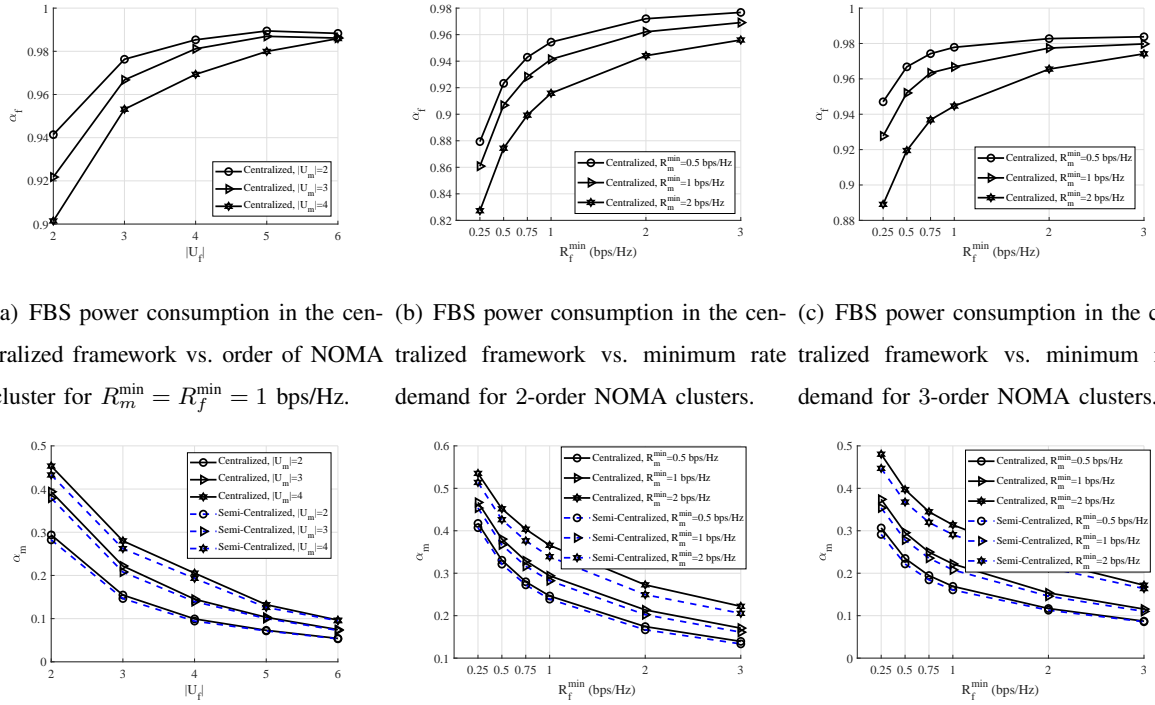


Fig. 4. Outage probability of the centralized and decentralized JSPA frameworks for different number of users and minimum rate demands.

significant higher total spectral efficiency, $\epsilon_\alpha = 10^{-2}$ is not good enough for calculating outage probability. ϵ_α can be easily reduced to 10^{-4} in the semi-centralized framework, however we set $\epsilon_\alpha = 10^{-2}$ for both the centralized and semi-centralized frameworks to have a fair comparison. For the same stepsize ϵ_α , the feasible region of the semi-centralized problem is a subset of the feasible region of its corresponding centralized problem.

2) *Total Spectral Efficiency Performance*: The performance of the decentralized frameworks depends on how good is the approximation of the power consumption of the BSs compared to the centralized framework. Figs. 5(a)-5(c) show the impact of order of NOMA clusters and



(a) FBS power consumption in the centralized framework vs. order of NOMA cluster for $R_m^{\min} = R_f^{\min} = 1$ bps/Hz. (b) FBS power consumption in the centralized framework vs. minimum rate demand for 2-order NOMA clusters. (c) FBS power consumption in the centralized framework vs. minimum rate demand for 3-order NOMA clusters.
(d) MBS power consumption in the centralized/semi-centralized frameworks vs. order of NOMA cluster for $R_f^{\min} = 1$ bps/Hz. (e) MBS power consumption in the centralized/semi-centralized frameworks vs. minimum rate demand for 2-order NOMA clusters. (f) MBS power consumption in the centralized/semi-centralized frameworks vs. minimum rate demand for 3-order NOMA clusters.

Fig. 5. Average power consumption coefficient of femto/macro BSs in the centralized/semi-centralized frameworks for different number of macro/femto-cell users and minimum rate demands.

minimum rate demands on the FBS power consumption coefficient α_f at the optimal point of the centralized framework. As is expected, larger $|\mathcal{U}_f|$ and/or R_f^{\min} results in larger FBS power consumption. Moreover, we observe that increasing $|\mathcal{U}_m|$ and/or R_m^{\min} decreases α_f . However, the impact of $|\mathcal{U}_m|$ and/or R_m^{\min} on α_f is quite low and negligible, due to the low ICI level from low-power FBS to macro-cell users in average. More importantly, we observe that in most of the cases, the FBS operates in up to 90% of its available power. It is noteworthy that in both the decentralized frameworks, we assume that the FBS operates in 100% of its available power. Figs. 5(d)-5(f) evaluate the impact of order of NOMA clusters and minimum rate demands on the MBS power consumption coefficient α_m at the optimal point of the centralized and semi-centralized frameworks. As is expected, α_m is directly proportional to $|\mathcal{U}_m|$ and/or R_m^{\min} , while is inversely proportional to $|\mathcal{U}_f|$ and/or R_f^{\min} . More importantly, we observe that

- 1) α_m in the semi-centralized framework is always upper-bounded by α_m in the centralized

framework. This is due to larger α_f in the semi-centralized framework compared to the centralized framework.

- 2) The MBS typically operates in less than 60% of its available power. Hence, the fully distributed framework with $\alpha_m = 1$ results in significantly degraded spectral efficiency at femto-cell users, due to high ICI from the MBS to femto-cell users.

Last but not least, we observe that the MBS power consumption gap between the centralized and semi-centralized frameworks is quite low (see Figs. 5(d)-5(f)).

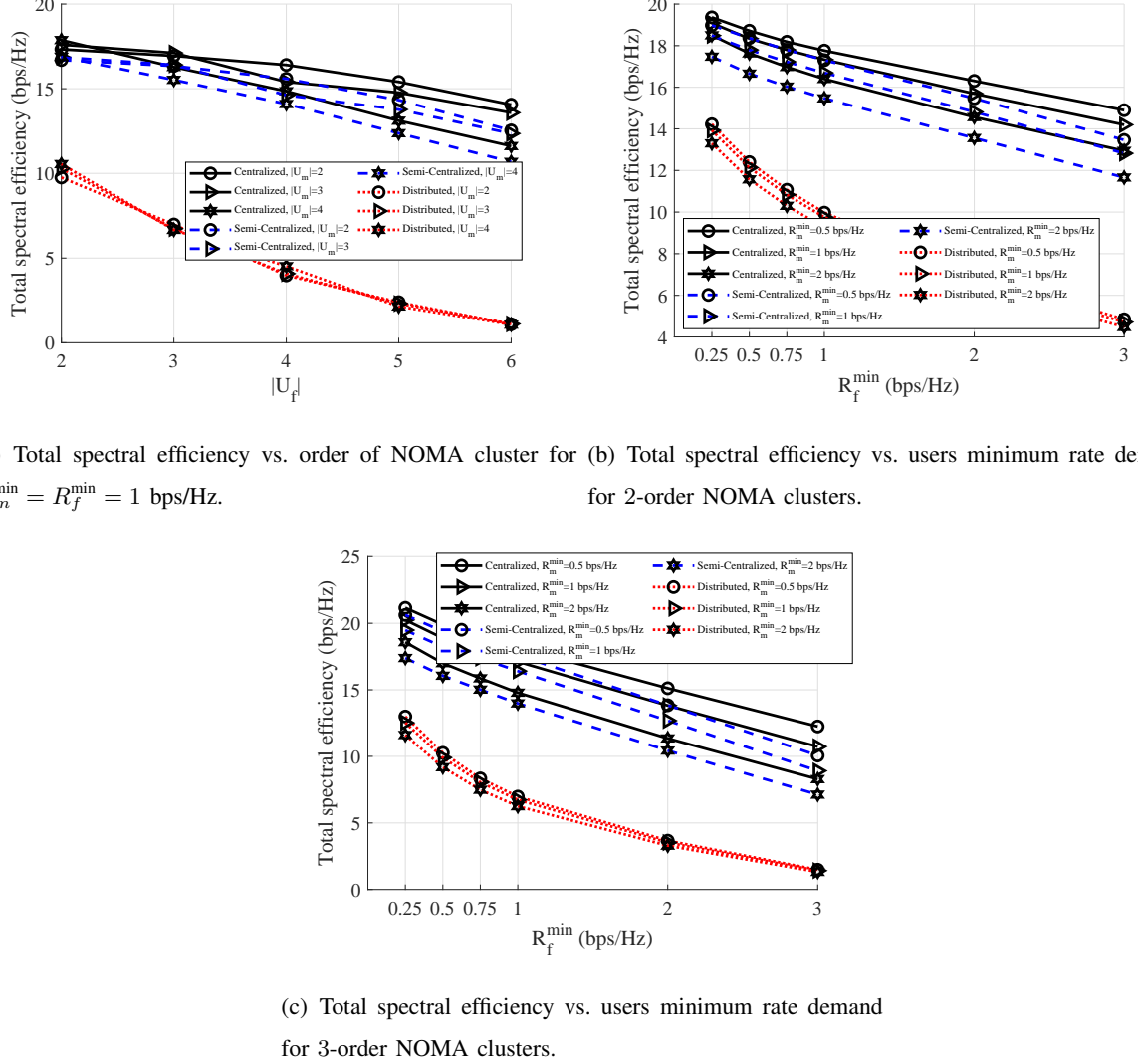
Fig. 6 investigates the total spectral efficiency of users in the centralized and decentralized frameworks. According to the discussions for Fig. 5, we observed that in most of the cases, the performance gap between the centralized (optimal) and semi-centralized frameworks is quite low, specifically for the lower order of the femto-cell NOMA cluster. Hence, the semi-centralized framework with its low computational complexity (see Table I) is a good candidate solution for the larger-scale systems. Besides, the fully distributed framework results in quite low performance, due to the discussions for Fig. 5.

D. Convergence of the Iterative Distributed Framework for Solving (10)

The feasible domain of problem (10) is empty if

- 1) Problem (10) is infeasible when the maximum power constraint (3b) is removed. This corresponds to the feasibility of (10) which can be determined by the Perron–Frobenius eigenvalues of the matrices arising from the power control subproblems (see Theorem 8 in [18]). In this theorem, it is proved that regardless of the availability of powers, (10) can be infeasible, due to the existing ICI and minimum rate demands.
- 2) Problem (10) is infeasible while (10) without (3b) is feasible. As a result, (10) is infeasible only because of the lack of power resources to meet the QoS constraints in (3c).

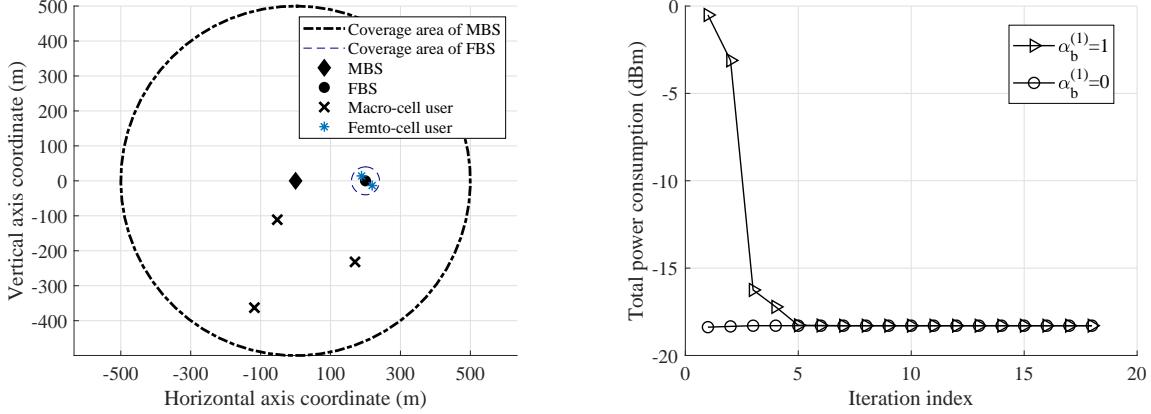
Since Alg. 2 is a component-wise minimum [18], for any feasible $\mathbf{p}^{(0)}$, it converges to a unique point which is the globally optimal solution. More importantly, the results show that Alg. 2 also converges to the globally optimal solution for any infeasible but finite $\mathbf{p}^{(0)}$ if the feasible domain of problem (10) is nonempty. Fig. 7(b) shows the convergence of Alg. 2 for different initial points. $\alpha_b^{(0)} = 0$ denotes a zero power consumption for the BSs, i.e., $p_{b,i}^{(0)} = 0, \forall b \in \mathcal{B}, i \in \mathcal{U}_b$. Besides, $\alpha_b^{(0)} = 1$ denotes that the BSs operate in their maximum power at the initial point which may violate (3c). Fig. 7(b) shows that Alg. 2 in both the initial points converges to the unique point. For $\alpha_b^{(0)} = 0$, the convergence of Alg. 2 corresponds tightening the lower-bound of optimal value,



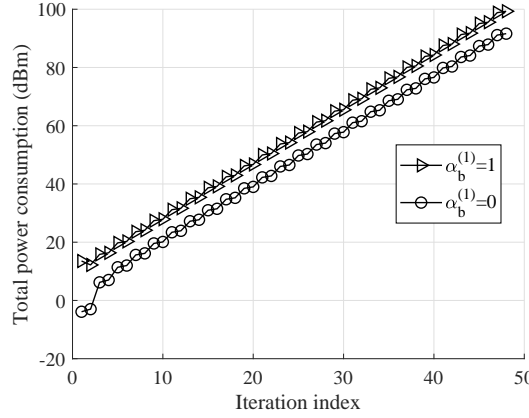
(a) Total spectral efficiency vs. order of NOMA cluster for (b) Total spectral efficiency vs. users minimum rate demand
 $R_m^{\min} = R_f^{\min} = 1$ bps/Hz. (c) Total spectral efficiency vs. users minimum rate demand for 2-order NOMA clusters.

Fig. 6. Total spectral efficiency of the centralized and decentralized frameworks for different number of macro/femto-cell users and minimum rate demands.

since the ICI at each user is always upper-bounded by its ICI at the converged point. Besides, since the ICI at each user reaches to its maximum possible value at $\alpha_b^{(0)} = 1$, the convergence of Alg. 2 for $\alpha_b^{(0)} = 1$ corresponds to tightening the upper-bound of optimal value. Based on the KKT conditions analysis in Appendix C, we observed that p^* is independent from the maximum power constraint (3b). It can be shown that if problem (10) is infeasible while (10) without (3b) is feasible (Case 2 of the infeasibility reasons of problem (10)), Alg. 2 will converge to the optimal finite point violating (3b). For larger minimum rate demands (Fig. 7(c)), we observe that Alg. 2 diverges and the optimal value tends to infinity, regardless of the maximum power



(a) The network topology and users placement for $|\mathcal{U}_m| = 3$, (b) Convergence of the iterative distributed framework for and $|\mathcal{U}_f| = 2$.
 $R_m^{\min} = 1$ bps/Hz, and $R_f^{\min} = 1$.



(c) Divergence of the iterative distributed framework for $R_m^{\min} = 4$ bps/Hz, and $R_f^{\min} = 4$.

Fig. 7. Convergence/Divergence of Alg. 2 for different initial points, and a channel realization with $|\mathcal{U}_m| = 3$, $|\mathcal{U}_f| = 2$, and different minimum rate demands.

constraint (3b). This corresponds to the first case of the infeasibility reasons of (10). Hence, it is important to check the Perron–Frobenius eigenvalues of the matrices arising from the power control subproblems (see Theorem 8 in [18]) before finding a feasible point for (10). Last but not least, Fig. 7(b) verifies a fast convergence speed of Alg. 2 for both the initialization methods, however $\alpha_b^{(0)} = 0$ converges in less iterations compared to $\alpha_b^{(0)} = 1$.

E. Convergence and Performance of the JRPA Algorithm

In Fig. 8, we investigate the convergence of our proposed JRPA algorithm which is based on sequential programming. We assume that the CNR-based decoding order is applied. Since the sequential programming converges to the locally optimal solution, the initial point may affect the performance of this method. In this study, we applied three initialization methods as

- 1) Minimum rate equality (MRE): In this method, we obtain $\mathbf{r}^{(0)}$ by solving the total power minimization problem (16). It is proved that at the optimal (feasible) point, the spectral efficiency of each user achieves its minimum rate demand. Hence, we have $r_{b,i}^{(0)} = R_{b,i}^{\min}, \forall b \in \mathcal{B}, i \in \mathcal{U}_b$.
- 2) Approximated rate function (ARF): In this method, we substitute the strictly concave term $g(r_{b,i}) = \ln(2^{r_{b,i}} - 1)$ with its approximated affine function $mr_{b,i}$ in (38c), where $m = \frac{\partial \ln(2^R - 1)}{\partial R}$, where R is significantly large. Then, we solve the convex approximated problem of (38) and obtain $\mathbf{r}^{(0)}$. For sufficiently large R , $g(r_{b,i})$ is upper-bounded by $m \times r_{b,i}$.
- 3) Equal power allocation (EPA): In this method, we equally distribute P_b^{\max} to all the users in \mathcal{U}_b , and then obtain $\mathbf{r}^{(0)}$ according to (2). This method may lead to an infeasible $\mathbf{r}^{(0)}$.

MRE provides a feasible $\mathbf{r}^{(0)}$. However, this method does not consider the heterogeneity of users spectral efficiency, leading to larger convergence speed and in some situations lower performance. MRE works well for the low-SINR scenarios with significantly high minimum rate demands. The ARF method provides a better feasible lower-bound for the total spectral efficiency of users at the initial point. Fig. 8(a) shows that for larger minimum rate demands, $\ln(2^r - 1) \approx mr$. The performance gap of ARF and the globally optimal solution is allocating more powers to users operating in low spectral efficiency regions, which results in allocating less power to the stronger user deserving additional power. ARF also works well for the scenarios that the low additional minimum rate demands does not have significant impact on the users total spectral efficiency, i.e., high SINR regions. The EPA initialization method usually leads to infeasible $\mathbf{r}^{(0)}$ violating (3c), due to INI and ICI at users. More importantly, we observed that EPA also leads to high outage at the next iteration of the JRPA algorithm. In Fig. 8, we selected the scenario that EPA (violating (3c)) does not make the next iteration infeasible to show the convergence behavior of this initialization method.

The users placement are shown in Fig. 8(b). As shown, the JRPA provides a sequence of

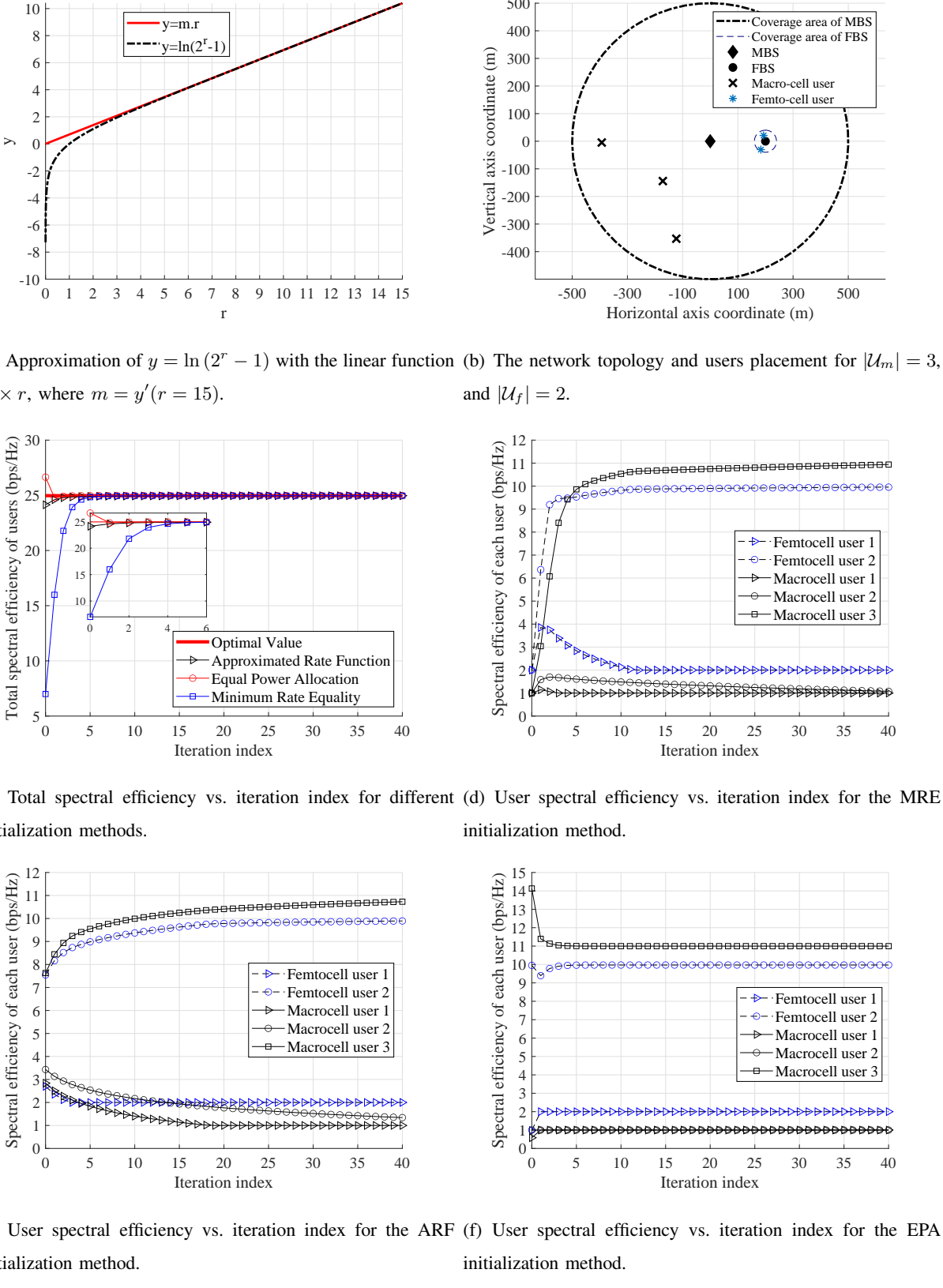


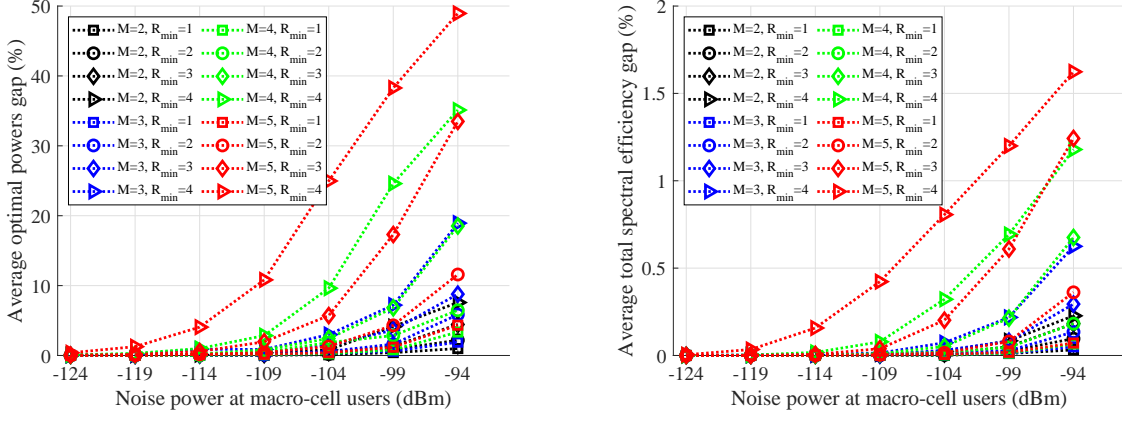
Fig. 8. Convergence of Alg. 3 for different initialization methods for a scenario with $|\mathcal{U}_m| = 3$, $|\mathcal{U}_f| = 2$, $R_m^{\min} = 1$ bps/Hz, and $R_f^{\min} = 2$. The CNR-based decoding order is optimal: Macro-cell users: $3 \rightarrow 2 \rightarrow 1$; Femto-cell users: $2 \rightarrow 1$.

improved solutions for any feasible initial point such that it converges to a stationary point. Interestingly, we observe that both the MRE and ARF methods converge to a unique point, which shows the low insensitivity of JRPA to these feasible initial points. In this scenario, EPA in iteration 0 results in infeasible $\mathbf{r}^{(0)}$. And, JRPA finds a feasible solution $\mathbf{r}^{(1)}$ based on infeasible $\mathbf{r}^{(0)}$, which is indeed the updated initial feasible point. According to Figs. 8(d)-8(f), we observe that at the converged point, only the NOMA cluster-head users get additional power (leading to higher spectral efficiency than their minimum rate demand). The fast convergence speed of individual rates in Figs. 8(d)-8(f) shows that our proposed JRPA has a fast convergence speed shown in Fig. 8(c). In our simulations, we applied the ARF initialization method.

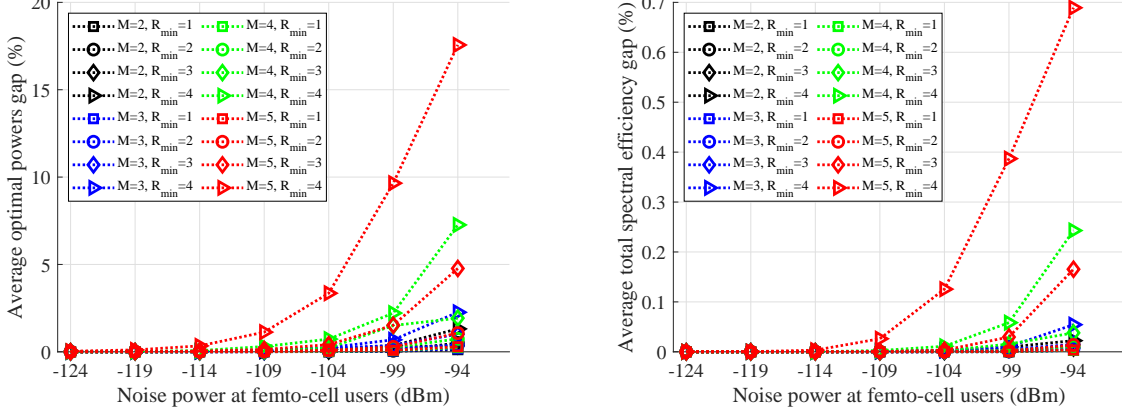
As is mentioned in Subsection III-A2, it is difficult to find the globally optimal JRPA for any fixed suboptimal decoding order. However, for the case that the fixed decoding order is the same as the optimal decoding order, the performance gap between the optimal JSPA and suboptimal JRPA algorithms is due to suboptimal JRPA based on sequential programming. In Fig. 8, we choosed the case that the CNR-based decoding order satisfy Theorem 1, so is optimal. The total spectral efficiency of users (optimal value) at the globally optimal point is shown in Fig. 8(c). As can be seen, the sequential programming generates a sequence of improved solutions such that after few iterations, it converges to a near-to-optimal solution.

F. Performance of the Approximated Optimal Powers in Remark III.2.1.

Here, we investigate the performance of approximated closed-form of optimal powers in Remark III.2.1. The advantage of this approximation is its insensitivity to the exact CSI. Fig. 9 compares the average gap between the exact and approximated forms of optimal powers in femto and macro-cells, separately. Since ICI is fully treated as AWGN, we evaluate this performance gap in different AWGN power levels of users which directly impacts the CINR of users. In Fig. 9, M is the number of users within the considered cell, and R_{\min} is their minimum rate demand. To reduce the randomness impact, we eliminated the Lognormal Shadowing from the path loss model (see Table II). As can be seen in Figs. 9(a) and 9(c), the average gap between the optimal and approximated powers is increasing in the order of NOMA clusters, minimum rate demands, and specifically AWGN power. Interestingly, for lower AWGN powers, e.g., less than -119 dBm, this performance gap tends to zero. As a result, this approximation works well for middle and high SINR scenarios. On the other hand, we observe that the macro/femto-cell total spectral efficiency gaps between these two closed-form formulations are less than 1.5% for



(a) Average optimal and approximated powers gap vs. AWGN power at macro-cell users. (b) Average total spectral efficiency gap vs. AWGN power at macro-cell users.



(c) Average optimal and approximated powers gap vs. AWGN power at femto-cell users. (d) Average total spectral efficiency gap vs. AWGN power at femto-cell users.

Fig. 9. The performance gap between the approximated and exact closed-form expression of optimal powers in macro/femto-cell for different AWGN powers, number of macro/femto-cell users, and minimum rate demands.

$M \leq 4$, $R_{\min} \leq 4$ bps/Hz, and AWGN power less than -94 dBm. Hence, the results show a high insensitivity level of optimal powers at macro/femto-cell users to the CSI. The impact of the approximated closed-form optimal powers on the ergodic rate regions and/or imperfect CSI can be considered as a future work.

V. CONCLUDING REMARKS

In this paper, we addressed the problem of optimal joint SIC ordering and power allocation in multi-cell NOMA systems to achieve the maximum users sum-rate. We showed that the optimal SIC ordering depends on the ICI at users. For the given total power consumption of BSs, we

obtained the optimal powers and SIC decoding orders in closed-form. Then, we proposed a globally optimal JSPA algorithm with a significantly reduced computational complexity. For any given suboptimal decoding order, we addressed the problem of joint rate and power allocation to maximize users sum-rate. We showed that for specific channel conditions, the CNR-based decoding order is optimal for a user pair. We also devised two decentralized resource allocation frameworks. Numerical assessments show that the optimal SIC ordering results in significantly lower outage probability and higher users sum-rate compared to the CNR-based decoding order. Moreover, for the fixed suboptimal SIC ordering, the rate adoption is necessary to achieve the maximum possible sum-rate. As a result, restricting the rate region of users results in high outage and subsequently seriously low sum-rate. Besides, we observed that the semi-centralized framework has a near-to-optimal performance with a significantly lower computational complexity compared to the globally optimal JSPA algorithm in the centralized framework.

APPENDIX A PROOF OF PROPOSITION III.1.

Let $\tilde{h}_{b,k} = \frac{h_{b,k}}{I_{b,k} + \sigma_{b,k}^2}$. The rate function in (2) can be reformulated as

$$R_{b,i} = \min_{k \in \{i\} \cup \Phi_{b,i}} \left\{ \log_2 \left(1 + \frac{p_{b,i} \tilde{h}_{b,k}}{\sum_{j \in \Phi_{b,i}} p_{b,j} \tilde{h}_{b,k} + 1} \right) \right\},$$

which is the same as the achievable rate of single-cell NOMA based on the equivalent noise. Since the SISO Gaussian broadcast channels are degraded [1], [2], NOMA with CINR-based decoding order is capacity achieving in each cell of multi-cell NOMA (where ICI is fully treated as AWGN), so the decoding order $\tilde{h}_{b,k} > \tilde{h}_{b,i} \Rightarrow k \rightarrow i$ is optimal [5], [10].

Similar to single-cell NOMA, in each cell b , we have $\frac{\partial \log_2 \left(1 + \frac{p_{b,k} \tilde{h}_{b,k}}{\sum_{j \in \Phi_{b,i}} p_{b,j} \tilde{h}_{b,k} + 1} \right)}{\partial \tilde{h}_{b,k}} > 0$. Assume that α_{-b} is fixed. In the following, we analytically show that at any given p_b (after linear superposition coding combined), the decoding order based on $\tilde{h}_{b,k}(\alpha_{-b}) > \tilde{h}_{b,i}(\alpha_{-b}) \Rightarrow k \rightarrow i$ achieves the maximum total spectral efficiency of users after SIC. Assume that cell b has M users. Moreover, the users index are updated based on $k > i$ if $\tilde{h}_{b,k}(\alpha_{-b}) > \tilde{h}_{b,i}(\alpha_{-b})$. We prove that the decoding order $M \rightarrow M-1 \rightarrow \dots \rightarrow 1$ outperforms any other possible decoding orders in terms of total spectral efficiency of users, so is optimal. To prove this, for two adjacent users i and $i+1$ (with $\tilde{h}_{b,i+1} > \tilde{h}_{b,i}$) consider different decoding orders as A) $i+1 \rightarrow i$, and

subsequently $M \rightarrow M-1 \rightarrow \dots \rightarrow 1$; B) $i \rightarrow i+1$, and subsequently $M \rightarrow M-1 \rightarrow \dots \rightarrow i+2 \rightarrow i \rightarrow i+1 \rightarrow i-1 \rightarrow \dots \rightarrow 1$. According to (2), the achievable spectral efficiency of users i and $i+1$ in case A (after SIC) can be obtained by

$$R_{b,i}^A(\mathbf{p}_b) = \log_2 \left(1 + \frac{p_{b,i} \tilde{h}_{b,i}}{\sum_{j=i+1}^M p_{b,j} \tilde{h}_{b,i} + 1} \right), \quad R_{b,i+1}^A(\mathbf{p}_b) = \log_2 \left(1 + \frac{p_{b,i+1} \tilde{h}_{b,i+1}}{\sum_{j=i+2}^M p_{b,j} \tilde{h}_{b,i+1} + 1} \right).$$

The achievable spectral efficiency of users i and $i+1$ in case B (after SIC) is given by

$$R_{b,i}^B(\mathbf{p}_b) = \log_2 \left(1 + \frac{p_{b,i} \tilde{h}_{b,i}}{\sum_{j=i+2}^M p_{b,j} \tilde{h}_{b,i} + 1} \right), \quad R_{b,i+1}^B(\mathbf{p}_b) = \log_2 \left(1 + \frac{p_{b,i+1} \tilde{h}_{b,i}}{(p_{b,i} + \sum_{j=i+2}^M p_{b,j}) \tilde{h}_{b,i} + 1} \right).$$

In both Cases A and B, the signal of users i and $i+1$ is treated as INI at users $1, \dots, i-1$. Moreover, the signal of users i and $i+1$ is scheduled to be decoded and canceled by all the users $i+2, \dots, M$. Hence, the set $\Phi_{b,k}$ of each user $k \in \{1, \dots, i-1, i+2, \dots, M\}$ is the same in both Cases A and B, resulting in the same spectral efficiency formulated in (2). Since the signal of all the users in \mathcal{U}_b is fully treated as noise (called ICI), the set $\Phi_{b',i}$ of each user $i \in \mathcal{U}_{b'}$, $b' \in \mathcal{B} \setminus \{b\}$ is the same in both the cases A and B resulting in the same spectral efficiency. Accordingly, changing the decoding order of two adjacent users only changes the capacity region of these two decoding orders for given \mathbf{p}_b . As a result, the total spectral efficiency gap between the different decoding orders A and B for given \mathbf{p}_b can be formulated by

$$\begin{aligned} R_{\text{gap}}^{A-B}(\mathbf{p}_b) &= \sum_{b \in \mathcal{B}} \sum_{i \in \mathcal{U}_b} R_{b,i}^A(\mathbf{p}_b) - \sum_{b \in \mathcal{B}} \sum_{i \in \mathcal{U}_b} R_{b,i}^B(\mathbf{p}_b) \\ &= (R_{b,i}^A(\mathbf{p}_b) + R_{b,i+1}^A(\mathbf{p}_b)) - (R_{b,i}^B(\mathbf{p}_b) + R_{b,i+1}^B(\mathbf{p}_b)) \\ &= \log_2 \left(\frac{\left(1 + \sum_{j=i}^M p_{b,j} \tilde{h}_{b,i} \right) \left(1 + \sum_{j=i+1}^M p_{b,j} \tilde{h}_{b,i+1} \right)}{\left(1 + \sum_{j=i+1}^M p_{b,j} \tilde{h}_{b,i} \right) \left(1 + \sum_{j=i+2}^M p_{b,j} \tilde{h}_{b,i+1} \right)} \right) + \\ &\quad \log_2 \left(\frac{\left(1 + \sum_{j=i+2}^M p_{b,j} \tilde{h}_{b,i} \right) \left(1 + (p_{b,i} + \sum_{j=i+2}^M p_{b,j}) \tilde{h}_{b,i} \right)}{\left(1 + (p_{b,i} + \sum_{j=i+2}^M p_{b,j}) \tilde{h}_{b,i} \right) \left(1 + \sum_{j=i}^M p_{b,j} \tilde{h}_{b,i} \right)} \right) \end{aligned}$$

$$\begin{aligned}
&= \log_2 \left(\frac{\left(1 + \sum_{j=i+1}^M p_{b,j} \tilde{h}_{b,i+1} \right) \left(1 + \sum_{j=i+2}^M p_{b,j} \tilde{h}_{b,i} \right)}{\left(1 + \sum_{j=i+1}^M p_{b,j} \tilde{h}_{b,i} \right) \left(1 + \sum_{j=i+2}^M p_{b,j} \tilde{h}_{b,i+1} \right)} \right) \\
&= \log_2 \left(\frac{1 + \left(\sum_{j=i+1}^M p_{b,j} \right) \tilde{h}_{b,i+1} + \left(\sum_{j=i+2}^M p_{b,j} \right) \tilde{h}_{b,i} + \left(\sum_{j=i+2}^M p_{b,j} \right) \left(\sum_{j=i+1}^M p_{b,j} \right) \tilde{h}_{b,i} \tilde{h}_{b,i+1}}{1 + \left(\sum_{j=i+1}^M p_{b,j} \right) \tilde{h}_{b,i} + \left(\sum_{j=i+2}^M p_{b,j} \right) \tilde{h}_{b,i+1} + \left(\sum_{j=i+2}^M p_{b,j} \right) \left(\sum_{j=i+1}^M p_{b,j} \right) \tilde{h}_{b,i} \tilde{h}_{b,i+1}} \right).
\end{aligned}$$

The difference of the numerator and denominator of the latter fraction is $p_{b,i+1} (\tilde{h}_{b,i+1} - \tilde{h}_{b,i})$, which is always positive since $\tilde{h}_{b,i+1} > \tilde{h}_{b,i}$, which results in $R_{\text{gap}}^{A-B}(\mathbf{p}_b) > 0$. Therefore, for any feasible \mathbf{p}_b , the decoding order $i+1 \rightarrow i$ for each two adjacent users i and $i+1$ in cell b is optimal if and only if $\tilde{h}_{b,i+1} > \tilde{h}_{b,i}$. Imposing this optimality condition to each two adjacent users in cell b results in the decoding order based on $\tilde{h}_{b,k}(\boldsymbol{\alpha}_{-b}) > \tilde{h}_{b,i}(\boldsymbol{\alpha}_{-b}) \Rightarrow k \rightarrow i$. As a result, $\lambda_{b,i,k}^* = 1$ if and only if $\tilde{h}_{b,i}(\boldsymbol{\alpha}_{-b}) \leq \tilde{h}_{b,k}(\boldsymbol{\alpha}_{-b})$, and the proof is completed.

APPENDIX B

PROOF OF PROPOSITION III.2.

According to Corollary III.1.1, the achievable spectral efficiency of each user $i \in \mathcal{U}_b$ for the fixed $\boldsymbol{\alpha}_{-b}$ and optimal decoding order $M \rightarrow M-1 \rightarrow \dots \rightarrow 1$ can be formulated by

$$\tilde{R}_{b,i}(\mathbf{p}_b) = \log_2 \left(1 + \frac{p_{b,i} \tilde{h}_{b,i}(\boldsymbol{\alpha}_{-b})}{\sum_{j=i+1}^M p_{b,j} \tilde{h}_{b,i}(\boldsymbol{\alpha}_{-b}) + 1} \right).$$

Note that $\tilde{h}_{b,k}(\boldsymbol{\alpha}_{-b}) > \tilde{h}_{b,i}(\boldsymbol{\alpha}_{-b})$ for each $i, k \in \mathcal{U}_b$, $k > i$. Moreover, $\tilde{R}_{b,i}$ is independent from \mathbf{p}_{-b} for given $\boldsymbol{\alpha}_{-b}$, meaning that (3) can be equivalently divided into B single-cell NOMA sub-problems. In cell b , we find \mathbf{p}_b^* by solving the following sub-problem as

$$\max_{\mathbf{p}_b \geq 0} \quad \sum_{i=1}^M \tilde{R}_{b,i}(\mathbf{p}_b) \quad (21a)$$

$$\text{s.t.} \quad \sum_{i \in \mathcal{U}_b} p_{b,i} = \alpha_b P_b^{\max}, \quad (21b)$$

$$\tilde{R}_{b,i}(\mathbf{p}_b) \geq R_{b,i}^{\min}, \quad \forall i \in \mathcal{U}_b. \quad (21c)$$

Similar to single-cell NOMA, it can be easily shown that the hessian of the sum-rate function in (21a) is negative definite in \mathbf{p}_b for $\tilde{h}_{b,k}(\boldsymbol{\alpha}_{-b}) > \tilde{h}_{b,i}(\boldsymbol{\alpha}_{-b})$ for each $i, k \in \mathcal{U}_b$, $k > i$ [11]–[13],

so the objective function (21a) is strictly concave on \mathbf{p}_b . (21c) can be rewritten as the following linear constraint $2^{R_{b,i}^{\min}} \left(1 + \sum_{j=i+1}^M p_{b,j} \tilde{h}_{b,i} \right) \leq 1 + \sum_{j=i}^M p_{b,j} \tilde{h}_{b,i}$. Hence, the feasible region of (21) is affine, so is convex. Accordingly, the problem (21) is strictly convex in \mathbf{p}_b . The Slater's condition holds in (21) since it is convex and there exists $\mathbf{p}_b \geq 0$ satisfying (21c) with strict inequalities. Therefore, the strong duality holds in (21). As a result, the KKT conditions are satisfied and the optimal solution \mathbf{p}^* can be obtained by using the Lagrange dual method [15]. The Lagrange function (upper-bound) of (21) is given by

$$L(\mathbf{p}_b, \boldsymbol{\mu}, \boldsymbol{\delta}, \nu) = \sum_{i=1}^M \log_2 \left(1 + \frac{p_{b,i} \tilde{h}_{b,i}}{1 + \sum_{j=i+1}^M p_{b,j} \tilde{h}_{b,i}} \right) + \sum_{i=1}^M \mu_i \left(\log_2 \left(1 + \frac{p_{b,i} \tilde{h}_{b,i}}{1 + \sum_{j=i+1}^M p_{b,j} \tilde{h}_{b,i}} \right) - R_{b,i}^{\min} \right) + \sum_{i=1}^M \delta_i p_{b,i} + \nu \left(\alpha_b P_b^{\max} - \sum_{i=1}^M p_{b,i} \right),$$

where $\boldsymbol{\mu} = [\mu_1, \dots, \mu_M]$, $\boldsymbol{\delta} = [\delta_1, \dots, \delta_M]$, and ν are the Lagrangian multipliers corresponding to the constraints (21c), (21b), and $p_{b,i} \geq 0$, $i = 1, \dots, M$, respectively. The Lagrange dual problem is given by

$$\begin{aligned} \min_{\boldsymbol{\mu}, \boldsymbol{\delta}, \nu} \quad & \sup_{\mathbf{p}} \{L(\mathbf{p}, \boldsymbol{\mu}, \boldsymbol{\delta}, \nu)\} \\ \text{s.t.} \quad & \mu_i \geq 0, \quad \forall i = 1, \dots, M, \\ & \delta_i \geq 0, \quad \forall i = 1, \dots, M. \end{aligned}$$

The KKT conditions are listed below:

1) Feasibility of the primal problem (21):

$$\mathbf{C-1.1:} \log_2 \left(1 + \frac{p_{b,i}^* \tilde{h}_{b,i}}{1 + \sum_{j=i+1}^M p_{b,j}^* \tilde{h}_{b,i}} \right) \geq R_{b,i}^{\min}, \quad \forall i, \quad \mathbf{C-1.2:} p_{b,i}^* \geq 0, \quad \forall i, \quad \mathbf{C-1.3:} \sum_{i=1}^M p_{b,i}^* = \alpha_b P_b^{\max}.$$

2) Feasibility of the dual problem:

$$\mathbf{C-2.1:} \mu_i^* \geq 0, \quad \forall i = 1, \dots, M, \quad \mathbf{C-2.2:} \delta_i^* \geq 0, \quad \forall i = 1, \dots, M, \quad \mathbf{C-2.3:} \nu^* \in \mathbb{R}.$$

3) The complementary slackness condition:

$$\mathbf{C-3.1:} \mu_i^* \left(\log_2 \left(1 + \frac{p_{b,i}^* \tilde{h}_{b,i}}{1 + \sum_{j=i+1}^M p_{b,j}^* \tilde{h}_{b,i}} \right) - R_{b,i}^{\min} \right) = 0, \forall i = 1, \dots, M,$$

$$\mathbf{C-3.2:} \delta_i^* p_{b,i}^* = 0, \forall i = 1, \dots, M.$$

4) The condition $\nabla_{\mathbf{p}_b^*} L(\mathbf{p}_b^*, \boldsymbol{\mu}^*, \boldsymbol{\delta}^*, \nu^*) = 0$, which implies that

$$\mathbf{C-4:} \frac{\partial L}{\partial p_{b,i}^*} = \sum_{k=1}^i \frac{1 + \mu_i^*}{\ln 2} \cdot \frac{\tilde{h}_{b,k}}{1 + \sum_{j=k}^M p_{b,j}^* \tilde{h}_{b,k}} - \sum_{k=1}^{i-1} \frac{1 + \mu_i^*}{\ln 2} \cdot \frac{\tilde{h}_{b,k}}{1 + \sum_{j=k+1}^M p_{b,j}^* \tilde{h}_{b,k}} + \delta_i^* - \nu^* = 0,$$

$$\forall i = 1, \dots, M.$$

This equation can be reformulated by

$$\frac{\partial L}{\partial p_{b,i}^*} = \frac{1 + \mu_i^*}{\ln 2} \cdot \frac{h_{b,1}}{1 + \sum_{j=1}^M p_{b,j}^* \tilde{h}_{b,1}} + \sum_{k=1}^{i-1} \frac{1 + \mu_i^*}{\ln 2} \cdot \left(\frac{\tilde{h}_{b,k+1}}{1 + \sum_{j=k+1}^M p_{b,j}^* \tilde{h}_{b,k+1}} - \frac{\tilde{h}_{b,k}}{1 + \sum_{j=k+1}^M p_{b,j}^* \tilde{h}_{b,k}} \right) +$$

$$\delta_i^* - \nu^* = 0, \forall i = 1, \dots, M.$$

To ease of convenience, we indicate $A(\mathbf{p}_b^*) = \frac{1}{\ln 2} \cdot \frac{\tilde{h}_{b,1}}{1 + \sum_{j=1}^M p_{b,j}^* \tilde{h}_{b,1}}$ and $B_k(\mathbf{p}_b^*) = \frac{1}{\ln 2} \cdot \frac{\tilde{h}_{b,k+1}}{1 + \sum_{j=k+1}^M p_{b,j}^* \tilde{h}_{b,k+1}} - \frac{\tilde{h}_{b,k}}{1 + \sum_{j=k+1}^M p_{b,j}^* \tilde{h}_{b,k}}$, $\forall k = 1, \dots, M-1$. Then, the last KKT condition can be reformulated as

$$\mathbf{C-4.1:} \frac{\partial L}{\partial p_{b,i}^*} = (1 + \mu_i^*) A(\mathbf{p}_b^*) + (1 + \mu_i^*) \sum_{k=1}^{i-1} B_k(\mathbf{p}_b^*) + \delta_i^* - \nu^* = 0, \forall i = 1, \dots, M. \quad (23)$$

The primal dual δ_i^* , $\forall i = 1, \dots, M$, acts as a slack variable in **C-4.1** (due to the KKT condition **C-2.2**), so it can be eliminated by reformulating the KKT conditions (**C-4.1**, **C-2.2**) and **C-3.2**, respectively as

$$\nu^* \geq (1 + \mu_i^*) \left(A(\mathbf{p}_b^*) + \sum_{k=1}^{i-1} B_k(\mathbf{p}_b^*) \right), \forall i = 1, \dots, M, \quad (24)$$

and

$$p_{b,i}^* \left(\nu^* - (1 + \mu_i^*) \left(A(\mathbf{p}_b^*) + \sum_{k=1}^{i-1} B_k(\mathbf{p}_b^*) \right) \right) = 0, \forall i = 1, \dots, M. \quad (25)$$

Obviously, $A(\mathbf{p}_b^*)$, $i = 1, \dots, M$, is positive at \mathbf{p}_b^* . According to Corollary III.1.1, $B_k(\mathbf{p}_b^*)$, $i = 1, \dots, M$, is also positive at \mathbf{p}_b^* , since $\tilde{h}_{b,k+1} > \tilde{h}_{b,k}$. To simplify the derivations, in the following,

we assume that $R_{b,i}^{\min} > 0$, $\forall i = 1, \dots, M$. Then, we show that the derivations are valid for the case than $R_{b,i}^{\min} = 0$ for some $i \in \mathcal{U}_b$. The assumption $R_{b,i}^{\min} > 0$, $\forall i = 1, \dots, M$ implies that $p_{b,i}^* > 0$, $\forall i = 1, \dots, M$ in **C-1.2**. According to (25), we have

$$\nu^* = (1 + \mu_i^*) \left(A(\mathbf{p}_b^*) + \sum_{k=1}^{i-1} B_k(\mathbf{p}_b^*) \right), \quad \forall i = 1, \dots, M. \quad (26)$$

Consider two adjacent users i and $i+1$. According to (26), we have

$$(1 + \mu_i^*) \left(A(\mathbf{p}_b^*) + \sum_{k=1}^{i-1} B_k(\mathbf{p}_b^*) \right) = (1 + \mu_{i+1}^*) \left(A(\mathbf{p}_b^*) + \sum_{k=1}^i B_k(\mathbf{p}_b^*) \right),$$

Since $A(\mathbf{p}_b^*) > 0$ and $B_k(\mathbf{p}_b^*) > 0, \forall k$, we have $A(\mathbf{p}_b^*) + \sum_{k=1}^i B_k(\mathbf{p}_b^*) > A(\mathbf{p}_b^*) + \sum_{k=1}^{i-1} B_k(\mathbf{p}_b^*)$. Accordingly, the latter equality holds if $\mu_{i+1}^* < \mu_i^*$. Therefore, there exists ν^* satisfying (26) if $\mu_{i+1}^* < \mu_i^*$ for each $i \in \mathcal{U}_b$. Accordingly, we have the following strict inequalities as

$$\mu_M^* < \mu_{M-1}^* < \dots < \mu_1^*.$$

Based on Condition **C-2.1**, we have $\mu_M^* \geq 0$ which implies that $\mu_i^* > 0$, $\forall i = 1, \dots, M-1$.

According to Condition **C-3.1**, the optimal power for users $1, \dots, M-1$ can be obtained by

$$\log_2 \left(1 + \frac{p_{b,i}^* \tilde{h}_{b,i}}{1 + \sum_{j=i+1}^M p_{b,j}^* \tilde{h}_{b,i}} \right) = R_{b,i}^{\min}, \quad \forall i = 1, \dots, M-1. \quad (27)$$

According to the power condition **C-1.3**, the optimal power of user M can be obtained by

$$p_{b,M}^* = \alpha_b P_b^{\max} - \sum_{i=1}^{M-1} p_{b,i}^*. \quad (28)$$

Note that $\mu_M^* > 0$ implies that $\log_2 \left(1 + p_{b,M}^* \tilde{h}_{b,M} \right) = R_{b,i}^{\min}$ due to Condition **C-3.1** which may violate Condition **C-1.3**. Therefore, at the optimal point $p_{b,M}^*$ obtained by (28), we have $\mu_M^* = 0$. Additionally, ν^* can take any value since at the optimal point, the KKT condition **C-1.3** holds. From (27), it can be concluded that at the optimal point \mathbf{p}_b^* , the allocated power to all the users with lower decoding order, i.e., users $i = 1, \dots, M-1$, is to only maintain their minimum spectral efficiency demand $R_{b,i}^{\min}$. Moreover, (28) proves that only the NOMA cluster-head user M deserves additional power. According to (27), the optimal power for each user $i < M$ can be obtained by

$$p_{b,i}^* = \frac{T_{b,i} \left(1 + \left(\alpha_b P_b^{\max} - \sum_{j=1}^{i-1} p_{b,j}^* \right) \tilde{h}_{b,i} \right)}{1 + T_{b,i} \tilde{h}_{b,i}}, \quad \forall i = 1, \dots, M-1, \quad (29)$$

where $T_i = \frac{2^{R_{b,i}^{\min}} - 1}{\tilde{h}_{b,i}}$, $\forall i = 1, \dots, M-1$. For the case that $R_{b,i}^{\min} \rightarrow 0$ for each user $i = 1, \dots, M-1$, then $T_{b,i} \rightarrow 0$. Therefore, $p_{b,i}^* \rightarrow 0$ meaning that when the spectral efficiency demand of the weaker user is zero, no power will be allocated to that user. According to (29), $p_{b,i}^*$ depends on optimal powers $p_{b,j}^*$, $\forall j = 1, \dots, i-1$. Hence, the optimal powers can be directly obtained by calculating $p_{b,1}^* \Rightarrow p_{b,2}^* \Rightarrow \dots \Rightarrow p_{b,M-1}^*$ by (29), and finally $p_{b,M}^*$ according to (28). To find a closed-form expression for $p_{b,i}^*$, we rewrite (29) as

$$p_{b,i}^* = \beta_{b,i} \left(P_b^{\max} - \sum_{j=1}^{i-1} p_{b,j}^* + \frac{1}{\tilde{h}_{b,i}} \right), \quad \forall i = 1, \dots, M-1,$$

where $\beta_{b,i} = \frac{2^{R_{b,i}^{\min}} - 1}{2^{R_{b,i}^{\min}}}$, $\forall i = 1, \dots, M-1$. Then, we have

$$\begin{aligned} p_{b,i}^* &= \beta_{b,i} \left(\alpha_b P_b^{\max} - p_{b,i-1}^* - \sum_{j=1}^{i-2} p_{b,j}^* + \frac{1}{\tilde{h}_{b,i}} \right) \\ &= \beta_{b,i} \left(\alpha_b P_b^{\max} - \beta_{b,i-1} \left(\alpha_b P_b^{\max} - \sum_{j=1}^{i-2} p_{b,j}^* + \frac{1}{\tilde{h}_{b,i-1}} \right) - \sum_{j=1}^{i-2} p_{b,j}^* + \frac{1}{\tilde{h}_{b,i}} \right) \\ &= \beta_{b,i} \left((1 - \beta_{b,i-1}) \alpha_b P_b^{\max} - (1 - \beta_{b,i-1}) \sum_{j=1}^{i-1} p_{b,j}^* + \frac{1}{\tilde{h}_{b,i}} - \frac{\beta_{b,i-1}}{\tilde{h}_{b,i-1}} \right) \\ &\quad \vdots \\ &= \beta_{b,i} \left((1 - \beta_{b,i-1}) (1 - \beta_{b,i-2}) \dots (1 - \beta_{b,1}) \alpha_b P_b^{\max} + \frac{1}{\tilde{h}_{b,i}} - \frac{\beta_{b,i-1}}{\tilde{h}_{b,i-1}} - \frac{(1 - \beta_{b,i-1}) \beta_{b,i-2}}{\tilde{h}_{b,i-2}} \dots \right. \\ &\quad \left. - \frac{(1 - \beta_{b,i-1}) (1 - \beta_{b,i-2}) \dots (1 - \beta_{b,2}) \beta_{b,1}}{\tilde{h}_{b,1}} \right). \end{aligned}$$

According to the above, we have

$$p_{b,i}^* = \beta_{b,i} \left(\prod_{j=1}^{i-1} (1 - \beta_{b,j}) \alpha_b P_b^{\max} + \frac{1}{\tilde{h}_{b,i}} - \sum_{j=1}^{i-1} \frac{\beta_{b,j} \prod_{k=j+1}^{i-1} (1 - \beta_{b,k})}{\tilde{h}_{b,j}} \right), \quad \forall i = 1, \dots, M-1.$$

According to (28), the optimal power of the NOMA cluster-head user M can be obtained by

$$p_{b,M}^* = \alpha_b P_b^{\max} - \sum_{i=1}^{M-1} \beta_{b,i} \left(\prod_{j=1}^{i-1} (1 - \beta_{b,j}) \alpha_b P_b^{\max} + \frac{1}{\tilde{h}_{b,i}} - \sum_{j=1}^{i-1} \frac{\beta_{b,j} \prod_{k=j+1}^{i-1} (1 - \beta_{b,k})}{\tilde{h}_{b,j}} \right).$$

APPENDIX C
CLOSED-FORM EXPRESSION OF OPTIMAL POWERS FOR TOTAL POWER MINIMIZATION
PROBLEM

Here, we first obtain the closed-form expression of optimal powers for a M -user single-cell NOMA system under the CNR-based decoding order. Then, we extend the results to the case that ICI is fixed in cell b serving M users and find the closed-form expressions of powers in \mathbf{p}_b^* under the CINR-based decoding order.

In the power minimization problem of a M -user single-cell NOMA system with $\tilde{h}_1 < \tilde{h}_2 < \dots < \tilde{h}_M$ and thus the optimal (CNR-based) decoding order $M \rightarrow M-1 \rightarrow \dots \rightarrow 1$, the achievable spectral efficiency of user i can be obtained by $R_i(\mathbf{p}) = \log_2 \left(1 + \frac{p_i \tilde{h}_i}{\sum_{j=i+1}^M p_j \tilde{h}_i + 1} \right)$. Here, $\tilde{h}_i = \frac{h_i}{\sigma_i^2}$ is the normalized channel gain of user i by its noise power σ_i^2 . The total power minimization problem under the CNR-based decoding order can be formulated by

$$\min_{\mathbf{p} \geq 0} \quad \sum_{i=1}^M p_i \quad (30a)$$

$$\text{s.t.} \quad \sum_{i=1}^M p_i \leq P^{\max}, \quad (30b)$$

$$\log_2 \left(1 + \frac{p_i \tilde{h}_i}{\sum_{j=i+1}^M p_j \tilde{h}_i + 1} \right) \geq R_i^{\min}, \quad \forall i = 1, \dots, M. \quad (30c)$$

The minimum rate constraint (30c) can be rewritten as $p_i h_i \geq (2^{R_i^{\min}} - 1) \left(\sum_{j=i+1}^M p_j \tilde{h}_i + 1 \right)$, $\forall i = 1, \dots, M$, which is affine in \mathbf{p} . Hence, problem (30) is convex in \mathbf{p} with an affine feasible set. It can be shown that in the power minimization problem, the allocated power to each user is only to maintain its minimal rate demand. In the following, we prove this proposition by analyzing the KKT conditions. The Slater's condition holds in (30) since it is convex and there exists $\mathbf{p} \geq 0$ satisfying (30b) and (30c) with strict inequalities. Therefore, the strong duality in (30) holds. Hence, the KKT conditions are satisfied and the optimal solution \mathbf{p}^* can be obtained by using the Lagrange dual method [15]. The Lagrange function (lower-bound) of (30) is given by

$$\begin{aligned}
L(\mathbf{p}, \boldsymbol{\mu}, \boldsymbol{\delta}, \nu) = & \sum_{i=1}^M p_i + \sum_{i=1}^M \mu_i \left(R_i^{\min} - \log_2 \left(1 + \frac{p_i \tilde{h}_i}{1 + \sum_{j=i+1}^M p_j \tilde{h}_i} \right) \right) + \sum_{i=1}^M \delta_i (-p_i) \\
& + \nu \left(\sum_{i=1}^M p_i - P^{\max} \right),
\end{aligned}$$

where $\boldsymbol{\mu} = [\mu_1, \dots, \mu_M]$, $\boldsymbol{\delta} = [\delta_1, \dots, \delta_M]$, and ν are the Lagrangian multipliers corresponding to the constraints (30c), (30b), and $p_i \geq 0$, $i = 1, \dots, M$, respectively. The Lagrange dual problem is given by

$$\begin{aligned}
\min_{\boldsymbol{\mu}, \boldsymbol{\delta}, \nu} \quad & \sup_{\mathbf{p}} \{L(\mathbf{p}, \boldsymbol{\mu}, \boldsymbol{\delta}, \nu)\} \\
\text{s.t.} \quad & \mu_i \geq 0, \quad \forall i = 1, \dots, M, \\
& \delta_i \geq 0, \quad \forall i = 1, \dots, M.
\end{aligned}$$

The KKT conditions are listed below.

1) Feasibility of the primal problem (30):

$$\mathbf{C-1.1:} \log_2 \left(1 + \frac{p_i^* \tilde{h}_i}{1 + \sum_{j=i+1}^M p_j^* \tilde{h}_i} \right) \geq R_i^{\min}, \quad \forall i, \quad \mathbf{C-1.2:} p_i^* \geq 0, \quad \forall i, \quad \mathbf{C-1.3:} \sum_{i=1}^M p_i^* \leq P^{\max}.$$

2) Feasibility of the dual problem:

$$\mathbf{C-2.1:} \mu_i^* \geq 0, \quad \forall i = 1, \dots, M, \quad \mathbf{C-2.2:} \delta_i^* \geq 0, \quad \forall i = 1, \dots, M, \quad \mathbf{C-2.3:} \nu^* \geq 0.$$

3) The complementary slackness condition:

$$\mathbf{C-3.1:} \mu_i^* \left(R_i^{\min} - \log_2 \left(1 + \frac{p_i^* \tilde{h}_i}{1 + \sum_{j=i+1}^M p_j^* \tilde{h}_i} \right) \right) = 0, \quad \forall i = 1, \dots, M,$$

$$\mathbf{C-3.2:} \delta_i^* p_i^* = 0, \quad \forall i = 1, \dots, M, \quad \mathbf{C-3.3:} \nu^* \left(\sum_{i=1}^M p_i^* - P^{\max} \right) = 0.$$

4) The condition $\nabla_{\mathbf{p}^*} L(\mathbf{p}^*, \boldsymbol{\mu}^*, \boldsymbol{\delta}^*, \nu^*) = 0$, which implies that

$$\mathbf{C-4:} \frac{\partial L}{\partial p_i^*} = 1 - \sum_{j=1}^{i-1} \mu_j^* \left(2^{R_j^{\min}} - 1 \right) \tilde{h}_j - \mu_i^* \tilde{h}_i - \delta_i^* + \nu^* = 0, \quad \forall i = 1, \dots, M.$$

Let $B_j = \left(2^{R_j^{\min}} - 1\right) \tilde{h}_j$, $j = 1, \dots, M$. The latter equation is rewritten as

$$\mathbf{C-4.1:} \frac{\partial L}{\partial p_i^*} = 1 - \sum_{j=1}^{i-1} \mu_j^* B_j - \mu_i^* \tilde{h}_i - \delta_i^* + \nu^* = 0, \quad \forall i = 1, \dots, M.$$

The primal dual δ_i^* , $\forall i = 1, \dots, M$, acts as a slack variable in **C-4.1** (due to the KKT condition **C-2.2**), so it can be eliminated by reformulating the KKT conditions (**C-4.1,C-2.2**) and **C-3.2**, respectively as

$$\nu^* \geq \sum_{j=1}^{i-1} \mu_j^* B_j + \mu_i^* \tilde{h}_i - 1, \quad \forall i = 1, \dots, M, \quad (32)$$

and

$$p_i^* \left(\nu^* - \left(\sum_{j=1}^{i-1} \mu_j^* B_j + \mu_i^* \tilde{h}_i - 1 \right) \right) = 0, \quad \forall i = 1, \dots, M. \quad (33)$$

We first assume that $R_i^{\min} > 0$, $\forall i = 1, \dots, M$. Then, we show that the derivations are valid for $R_i^{\min} = 0$ for some i . The assumption $R_i^{\min} > 0$, $\forall i = 1, \dots, M$ implies that $p_i^* > 0$, $\forall i = 1, \dots, M$ in **C-1.2**. According to (33), we have

$$\nu^* = \sum_{j=1}^{i-1} \mu_j^* B_j + \mu_i^* \tilde{h}_i - 1, \quad \forall i = 1, \dots, M. \quad (34)$$

Consider two adjacent users i and $i + 1$. According to (34), we have

$$\sum_{j=1}^{i-1} \mu_j^* B_j + \mu_i^* \tilde{h}_i = \left(\sum_{j=1}^{i-1} \mu_j^* B_j + \mu_i^* B_i \right) + \mu_{i+1}^* h_{i+1},$$

which can be simplified to

$$\mu_i^* \tilde{h}_i = \mu_i^* B_i + \mu_{i+1}^* h_{i+1} \quad \Rightarrow \quad \mu_i^* \left(\tilde{h}_i - B_i \right) = \mu_{i+1}^* h_{i+1}.$$

In the following, we prove that $\mu_{i+1}^* < \mu_i^*$. Let $\mu_{i+1}^* \geq \mu_i^*$. It implies that $h_{i+1} \leq \tilde{h}_i - B_i$, which is equivalent to $h_{i+1} + B_i \leq \tilde{h}_i$. Since $B_i > 0$, it results in $h_{i+1} \leq \tilde{h}_i$ which violates our assumption $h_{i+1} > \tilde{h}_i$. Accordingly, (34) holds if $\mu_{i+1}^* < \mu_i^*$ for each two adjacent users i and $i + 1$. Hence, there exists ν^* satisfying (34) if

$$\mu_M^* < \mu_{M-1}^* < \dots < \mu_1^*.$$

According to Condition **C-2.1**, we have $\mu_M^* \geq 0$ which implies that $\mu_i^* > 0$, $\forall i = 1, \dots, M - 1$. The optimal Lagrangian multiplier μ_M^* of the NOMA cluster-head user is also positive. This is due to the fact that $r_M(p_M^*) = \log_2(1 + p_M^* h_M)$ in (30c) is monotonically increasing in p_M^* , and also independent from the other optimal powers. Hence, at the optimal point which corresponds

to the minimal p_M^* , the spectral efficiency $r_M(p_M^*)$ reaches to its lower-bound R_M^{\min} . Hence, we have $\log_2(1 + p_M^* h_M) = R_M^{\min}$. According to the KKT condition **C-3.1**, $\mu_M^* > 0$. As a result, we have

$$0 < \mu_M^* < \mu_{M-1}^* < \cdots < \mu_1^*.$$

According to Condition **C-3.1**, the optimal power for each user $i = 1, \dots, M$ can be obtained by

$$\log_2 \left(1 + \frac{p_i^* \tilde{h}_i}{1 + \sum_{j=i+1}^M p_j^* \tilde{h}_i} \right) = R_i^{\min}, \quad \forall i = 1, \dots, M. \quad (35)$$

It is noteworthy that the duality gap between the primal and dual problems is zero when the Slater's condition holds. This condition implies that there exists \mathbf{p} such that the KKT condition **C-1.3** with strict inequality holds, meaning that the feasible region of (30) with strict inequality power constraint $\sum_{i=1}^M p_i < P^{\max}$ is nonempty. Since $\sum_{i=1}^M p_i = P^{\max}$ corresponds to the maximum value of the objective function (30a), satisfying the Slater's condition ensures us $\sum_{i=1}^M p_i^* < P^{\max}$. According to Condition **C-3.3**, we have¹¹ $\nu^* = 0$. According to the above, it can be concluded that at the optimal point \mathbf{p}^* , the allocated power to each user i is only to maintain its minimum spectral efficiency demand R_i^{\min} . According to (27), the optimal power (in Watts) for each user $i < M$ can be obtained by

$$p_i^* = T_i \left(1 + \sum_{j=i+1}^M p_j^* \tilde{h}_i \right), \quad \forall i = 1, \dots, M, \quad (36)$$

where $T_i = \frac{2^{R_i^{\min}} - 1}{\tilde{h}_i}$, $\forall i = 1, \dots, M$. For the case that $R_i^{\min} \rightarrow 0$, then $T_i \rightarrow 0$. Therefore, $p_i^* \rightarrow 0$ meaning that no power will be allocated to user i . Similar to (29), it can be easily shown that the optimal powers can be obtained directly by (36). To obtain a closed-form expression for p_i^* , we rewrite (36) as

$$p_i^* = \beta_i \left(\frac{1}{\tilde{h}_i} + \sum_{j=i+1}^M p_j^* \right), \quad \forall i = 1, \dots, M,$$

where $\beta_i = 2^{R_i^{\min}} - 1$, $\forall i = 1, \dots, M$. The optimal power p_i^* can be reformulated as

$$p_i^* = \beta_i \left(\frac{1}{\tilde{h}_i} + \sum_{j=i+1}^M p_j^* \right)$$

¹¹The discussions about optimal $\nu^* = 0$ is only additional notes on the impact of the power constraint. We proved that for any non-empty feasible set satisfying the Slater's condition, the power constraint will not be active.

$$\begin{aligned}
&= \beta_i \left(\frac{1}{\tilde{h}_i} + p_{i+1}^* + \sum_{j=i+2}^M p_j^* \right) \\
&= \beta_i \left(\frac{1}{\tilde{h}_i} + \beta_{i+1} \left(\frac{1}{\tilde{h}_{i+1}} + \sum_{j=i+2}^M p_j^* \right) + \sum_{j=i+2}^M p_j^* \right) \\
&= \beta_i \left((1 + \beta_{i+1}) \sum_{j=i+2}^M p_j^* + \frac{1}{\tilde{h}_i} + \frac{\beta_{i+1}}{h_{i+1}} \right) \\
&= \beta_i \left((1 + \beta_{i+1}) \left(p_{i+2}^* + \sum_{j=i+3}^M p_j^* \right) + \frac{1}{\tilde{h}_i} + \frac{\beta_{i+1}}{h_{i+1}} \right) \\
&= \beta_i \left((1 + \beta_{i+1}) \left(\beta_{i+2} \left(\frac{1}{\tilde{h}_{i+2}} + \sum_{j=i+3}^M p_j^* \right) + \sum_{j=i+3}^M p_j^* \right) + \frac{1}{\tilde{h}_i} + \frac{\beta_{i+1}}{h_{i+1}} \right) \\
&= \beta_i \left((1 + \beta_{i+1})(1 + \beta_{i+2}) \sum_{j=i+3}^M p_j^* + \frac{1}{\tilde{h}_i} + \frac{\beta_{i+1}}{h_{i+1}} + \frac{\beta_{i+2}(1 + \beta_{i+1})}{h_{i+2}} \right) \\
&\vdots \\
&= \beta_i \left((1 + \beta_{i+1})(1 + \beta_{i+2}) \dots (1 + \beta_M) + \frac{1}{\tilde{h}_i} + \frac{\beta_{i+1}}{h_{i+1}} + \frac{\beta_{i+2}(1 + \beta_{i+1})}{h_{i+2}} + \dots \right. \\
&\quad \left. + \frac{\beta_M(1 + \beta_{M-1}) \dots (1 + \beta_{i+1})}{h_M} \right).
\end{aligned}$$

According to the above, we have

$$p_i^* = \beta_i \left(\prod_{j=i+1}^M (1 + \beta_j) + \frac{1}{\tilde{h}_i} + \sum_{j=i+1}^M \frac{\beta_j \prod_{k=i+1}^{j-1} (1 + \beta_k)}{\tilde{h}_j} \right), \quad \forall i = 1, \dots, M. \quad (37)$$

In multi-cell NOMA, let cell b has M users with $\tilde{h}_{b,1} < \tilde{h}_{b,2} < \dots < \tilde{h}_{b,M}$, where $\tilde{h}_{b,i} = \frac{h_{b,i}}{I_{b,i} + \sigma_{b,i}^2}$. According to Corollary III.1.1, the achievable spectral efficiency of each user $i \in \mathcal{U}_b$ under the optimal decoding order $M \rightarrow M-1 \rightarrow \dots \rightarrow 1$ is $\tilde{R}_{b,i}(\mathbf{p}) = \log_2 \left(1 + \frac{p_{b,i} \tilde{h}_{b,i}}{\sum_{j=i+1}^M p_{b,j} \tilde{h}_{b,j} + 1} \right)$.

In multi-cell NOMA, for the case that ICI is fixed, the power minimization problem of cell b under the optimal (CINR-based) decoding order corresponds to the power minimization problem of single-cell NOMA. According to (37), for the case that $\tilde{h}_{b,1} < \tilde{h}_{b,2} < \dots < \tilde{h}_{b,M}$, the optimal power of each user $i \in \mathcal{U}_b$ can be obtained in closed form as

$$p_{b,i}^* = \beta_{b,i} \left(\prod_{j=i+1}^M (1 + \beta_{b,j}) + \frac{1}{\tilde{h}_{b,i}} + \sum_{j=i+1}^M \frac{\beta_{b,j} \prod_{k=i+1}^{j-1} (1 + \beta_{b,k})}{\tilde{h}_{b,j}} \right), \quad \forall i = 1, \dots, M.$$

APPENDIX D

JOINT POWER ALLOCATION AND RATE ADOPTION ALGORITHM

By taking \ln from the both sides of (14c), we have $\ln(2^{r_{b,i}} - 1) + \ln \left(\sum_{j \in \Phi_{b,i}} p_{b,j} h_{b,k} + I_{b,k} + \sigma_{b,k}^2 \right) \leq \ln(p_{b,i} h_{b,k}), \forall b \in \mathcal{B}, i, k \in \mathcal{U}_b, k \in \{i\} \cup \Phi_{b,i}$. Now, let $p_{b,i} = e^{\tilde{p}_{b,i}}$, and subsequently $I_{b,i}(\tilde{\mathbf{p}}_{-b}) = \sum_{j \in \mathcal{B}, j \neq b} \left(\sum_{l \in \mathcal{U}_j} e^{\tilde{p}_{j,l}} \right) h_{j,b,i}$. Accordingly, problem (3) can be rewritten as

$$\max_{\tilde{\mathbf{p}}, \mathbf{r} \geq 0} \quad \sum_{b \in \mathcal{B}} \sum_{i \in \mathcal{U}_b} r_{b,i} \quad (38a)$$

s.t. (14b),

$$\sum_{i \in \mathcal{U}_b} e^{\tilde{p}_{b,i}} \leq P_b^{\max}, \forall b \in \mathcal{B}, \quad (38b)$$

$$\ln(2^{r_{b,i}} - 1) + \ln \left(\sum_{j \in \Phi_{b,i}} e^{\tilde{p}_{b,j}} h_{b,k} + \sum_{j \in \mathcal{B}, j \neq b} \left(\sum_{l \in \mathcal{U}_j} e^{\tilde{p}_{j,l}} \right) h_{j,b,i} + \sigma_{b,k}^2 \right) \leq \tilde{p}_{b,i} \ln(h_{b,k}),$$

$$\forall b \in \mathcal{B}, i, k \in \mathcal{U}_b, k \in \{i\} \cup \Phi_{b,i}. \quad (38c)$$

The objective function (38) is affine, so is concave on \mathbf{r} . Constraint (14b) is affine, so is convex. Constraint (38b) is also convex since log-sum-exp is convex [15]. However, (38c) is nonconvex. In the left hand side of (38c), it can be easily shown that the first term $\ln(2^{r_{b,i}} - 1)$ is strictly concave on $r_{b,i}$ which makes (38) nonconvex and strongly NP-hard. Now, we apply the iterative sequential programming method. At each iteration t , we approximate the term $g(r_{b,i}^{(t)}) = \ln(2^{r_{b,i}^{(t)}} - 1)$ to its first-order Taylor series around $r_{b,i}^{(t-1)}$ obtained from prior iteration $(t-1)$ as follows:

$$\hat{g}(r_{b,i}^{(t)}) = g(r_{b,i}^{(t-1)}) + g'(r_{b,i}^{(t-1)}) (r_{b,i}^{(t)} - r_{b,i}^{(t-1)}), \quad (39)$$

where $g'(r) = \frac{2r}{2^r - 1}$. By substituting $g(r_{b,i}^{(t)})$ with its affine approximated form $\hat{g}(r_{b,i}^{(t)})$ in (39), problem (38) at iteration t will be approximated to the following convex form as

$$\max_{\tilde{\mathbf{p}}^{(t)}, \mathbf{r}^{(t)} \geq 0} \quad \sum_{b \in \mathcal{B}} \sum_{i \in \mathcal{U}_b} r_{b,i}^{(t)} \quad (40a)$$

s.t. (14b), (38b)

$$\hat{g}(r_{b,i}^{(t)}) + \ln \left(\sum_{j \in \Phi_{b,i}} e^{\tilde{p}_{b,j}^{(t)}} h_{b,k} + \sum_{j \in \mathcal{B}, j \neq b} \left(\sum_{l \in \mathcal{U}_j} e^{\tilde{p}_{j,l}^{(t)}} \right) h_{j,b,i} + \sigma_{b,k}^2 \right) \leq \tilde{p}_{b,i}^{(t)} \ln(h_{b,k}), \forall b \in \mathcal{B},$$

$$i, k \in \mathcal{U}_b, k \in \{i\} \cup \Phi_{b,i}. \quad (40b)$$

It can be shown that (40) satisfies the KKT conditions [29], so it can be solved by using the Lagrange dual method, or IPMs [15]. In the sequential programming, we first initialize $\mathbf{r}^{(0)}$. At each iteration t , we solve (40) and find $(\mathbf{r}^{*(t)}, \tilde{\mathbf{p}}^{*(t)})$ according to the updated $\hat{g}(r_{b,i}^{(t)})$ based on $\mathbf{r}^{*(t-1)}$. We continue the iterations until the convergence is achieved.

The solution of (40) remains in the feasible region of the main problem (38). This is due to the fact that at each iteration t , we have $\hat{g}(r_{b,i}^{(t)}) \geq g(r_{b,i}^{(t)})$. Let $(\hat{\mathbf{r}}^{(t)}, \hat{\mathbf{p}}^{(t)})$ be the feasible solution of (40). It implies that (40b) is satisfied. Thus, we have

$$\hat{p}_{b,i}^{(t)} \ln(h_{b,k}) - \ln \left(\sum_{j \in \Phi_{b,i}} e^{\hat{p}_{b,j}^{(t)}} h_{b,k} + \sum_{\substack{j \in \mathcal{B} \\ j \neq b}} \left(\sum_{l \in \mathcal{U}_j} e^{\hat{p}_{j,l}^{(t)}} \right) h_{j,b,i} + \sigma_{b,k}^2 \right) \geq \hat{g}(\hat{r}_{b,i}^{(t)}), \quad \forall b \in \mathcal{B},$$

$$i, k \in \mathcal{U}_b, k \in \{i\} \cup \Phi_{b,i}.$$

Since $\hat{g}(r_{b,i}^{(t)}) \geq g(r_{b,i}^{(t)})$, we can guarantee that (38c) is satisfied, meaning that (40) remains in the feasible region of (38). It can be easily shown that the sequential programming generates a sequence of improved feasible solutions, such that it converges to a stationary point which is a local maxima of (38) [29]. The performance and convergence of this algorithm is numerically evaluated in Subsection IV-E.

APPENDIX E

PROOF OF THEOREM 1.

For each user pair $i, k \in \mathcal{U}_b$, if (4) holds at any power level \mathbf{p}_{-b} , the decoding order $k \rightarrow i$ is optimal. Note that (4) for cell b is completely independent from \mathbf{p}_b (see Proposition III.1). Let us rewrite (4) for the user pair $i, k \in \mathcal{U}_b$ as

$$\frac{h_{b,k}}{\sigma_{b,k}} - \frac{h_{b,i}}{\sigma_{b,i}} \geq \sum_{\substack{j \in \mathcal{B} \\ j \neq b}} \frac{\left(\sum_{i \in \mathcal{U}_b} p_{j,i} \right)}{\sigma_{b,i} \sigma_{b,k}} (h_{j,b,k} h_{b,i} - h_{j,b,i} h_{b,k}). \quad (41)$$

For the case that the left-hand side (LHS) is non-negative and each term in the right-hand side (RHS) is non-positive, (41) is satisfied at any power level \mathbf{p}_{-b} [20]. These conditions imply that with $\frac{h_{b,k}}{\sigma_{b,k}} \geq \frac{h_{b,i}}{\sigma_{b,i}}$ and $\frac{h_{b,k}}{h_{b,i}} \geq \frac{h_{j,b,k}}{h_{j,b,i}}$, $\forall j \in \mathcal{B} \setminus \{b\}$, the decoding order $k \rightarrow i$ is optimal. Now, assume that for BSs in $\mathcal{Q}_{b,i,k} \subseteq \mathcal{B} \setminus \{b\}$ we have $h_{j,b,k} h_{b,i} - h_{j,b,i} h_{b,k} > 0$. Moreover, each BS $j \in \mathcal{Q}_{b,i,k}$ operates at its maximum power P_j^{\max} , meaning that $\sum_{i \in \mathcal{U}_b} p_{j,i} = P_j^{\max}$, $\forall j \in \mathcal{Q}_{b,i,k}$. In

the following, we show that if $\frac{h_{b,k}}{\sigma_{b,k}} - \frac{h_{b,i}}{\sigma_{b,i}} \geq \sum_{j \in \mathcal{Q}_{b,i,k}} \frac{P_j^{\max}}{\sigma_{b,i}\sigma_{b,k}} (h_{j,b,k}h_{b,i} - h_{j,b,i}h_{b,k})$, the inequality (41) holds for any power level \mathbf{p}_{-b} . To prove this, we first note that the inequality

$$\sum_{j \in \mathcal{Q}_{b,i,k}} \frac{P_j^{\max}}{\sigma_{b,i}\sigma_{b,k}} (h_{j,b,k}h_{b,i} - h_{j,b,i}h_{b,k}) \geq \sum_{j \in \mathcal{Q}_{b,i,k}} \frac{\left(\sum_{i \in \mathcal{U}_b} p_{j,i} \right)}{\sigma_{b,i}\sigma_{b,k}} (h_{j,b,k}h_{b,i} - h_{j,b,i}h_{b,k}), \quad (42)$$

always holds since $(h_{j,b,k}h_{b,i} - h_{j,b,i}h_{b,k})$ is positive for each BS $j \in \mathcal{Q}_{b,i,k}$, and $\sum_{i \in \mathcal{U}_b} p_{j,i} \leq P_j^{\max}$, $\forall j \in \mathcal{Q}_{b,i,k}$. On the other hand, for each BS $j' \in \mathcal{B} \setminus \{\mathcal{Q}_{b,i,k} \cup \{b\}\}$, we have $(h_{j,b,k}h_{b,i} - h_{j,b,i}h_{b,k}) \leq 0$. Accordingly, if $\frac{h_{b,k}}{\sigma_{b,k}} \geq \frac{h_{b,i}}{\sigma_{b,i}}$ and (42) holds, the inequality in (41) holds for any power level \mathbf{p}_{-b} , so the decoding order $k \rightarrow i$ is optimal at any feasible \mathbf{p}_{-b} .

APPENDIX F

PROOF OF FACT III.2.1.

For convenience, let all the channel gains be normalized by noise. According to (41), for each user pair $i, k \in \mathcal{U}_b$, $k \in \Phi_{b,i}$, (17) can be rewritten as the following linear constraint:

$$h_{b,k} - h_{b,i} \geq \sum_{\substack{j \in \mathcal{B} \\ j \neq b}} \left(\sum_{i \in \mathcal{U}_b} p_{j,i} \right) (h_{j,b,k}h_{b,i} - h_{j,b,i}h_{b,k}). \quad (43)$$

Constraint (43) can be equivalently transformed to $(B-1)$ maximum power constraints including all the BSs in $\mathcal{B} \setminus \{b\}$. The power consumption of each BS $j \in \mathcal{B} \setminus \{b\}$ is upper-bounded by

$$\sum_{i \in \mathcal{U}_b} p_{j,i} \leq \underbrace{\frac{(h_{b,k} - h_{b,i}) - \sum_{l \in \mathcal{B} \setminus \{j,b\}} \left(\sum_{i \in \mathcal{U}_b} p_{l,i} \right) (h_{l,b,k}h_{b,i} - h_{l,b,i}h_{b,k})}{h_{j,b,k}h_{b,i} - h_{j,b,i}h_{b,k}}}_{\Psi_{j,b,i,k}(\mathbf{p}_{-(j,b)})}. \quad (44)$$

In general, the maximum power constraint (3b) and SIC constraint (17) can be equivalently combined as

$$\sum_{i \in \mathcal{U}_b} p_{b,i} \leq \min \left\{ P_b^{\max}, \min_{\substack{j \in \mathcal{B} \setminus \{b\}, \\ i, k \in \mathcal{U}_j, k \in \Phi_{j,i}}} \Psi_{b,j,i,k}(\mathbf{p}_{-(b,j)}) \right\}, \quad \forall b \in \mathcal{B}. \quad (45)$$

The negative side impact of the SIC necessary constraint (17) can be observed in (45). For the case that $\min_{\substack{j \in \mathcal{B} \setminus \{b\}, \\ i, k \in \mathcal{U}_j, k \in \Phi_{j,i}}} \Psi_{b,j,i,k}(\mathbf{p}_{-(b,j)}) < P_b^{\max}$, (17) imposes additional limitations on the total power consumption of BS b which restricts the feasible region of (3b).

APPENDIX G

PROOF OF FACT III.2.2.

In the sum-rate maximization problem of a M -user single-cell NOMA system with normalized channel gains $h_1 < h_2 < \dots < h_M$, and thus optimal (CNR-based) decoding order $M \rightarrow M-1 \rightarrow \dots \rightarrow 1$, the achievable spectral efficiency of user i can be obtained by $R_i(\mathbf{p}) = \log_2 \left(1 + \frac{p_i h_i}{\sum_{j=i+1}^M p_j h_{i+1}} \right)$. The sum-rate function $\sum_{i=1}^M \log_2 \left(1 + \frac{p_i h_i}{\sum_{j=i+1}^M p_j h_{i+1}} \right)$ is monotonically increasing in p_1 , i.e., the allocated power to user 1 with the lowest decoding order. In fact, the signal of user 1 with lowest decoding order is decoded and canceled by all the other users $i = 2, \dots, M$. Due to the power constraint $\sum_{i=1}^M p_i \leq P^{\max}$, and the fact that $R_1(\mathbf{p})$ is monotonically increasing in p_1 , at the optimal point \mathbf{p}^* , we have $p_1^* = P^{\max} - \sum_{i=2}^M p_i^*$. In other words, we ensure that at the optimal point, we have $\sum_{i=1}^M p_i^* = P^{\max}$, and the proof is completed.

REFERENCES

- [1] H. Weingarten, Y. Steinberg, and S. S. Shamai, “The capacity region of the Gaussian multiple-input multiple-output broadcast channel,” *IEEE Transactions on Information Theory*, vol. 52, no. 9, pp. 3936–3964, 2006.
- [2] A. E. Gamal and Y.-H. Kim, *Network Information Theory*. Cambridge University Press, 2011.
- [3] Y. Saito, Y. Kishiyama, A. Benjebbour, T. Nakamura, A. Li, and K. Higuchi, “Non-orthogonal multiple access (NOMA) for cellular future radio access,” in *Proc. IEEE 77th Vehicular Technology Conference (VTC Spring)*, 2013, pp. 1–5.
- [4] Z. Ding, X. Lei, G. K. Karagiannidis, R. Schober, J. Yuan, and V. K. Bhargava, “A survey on non-orthogonal multiple access for 5G networks: Research challenges and future trends,” *IEEE Journal on Selected Areas in Communications*, vol. 35, no. 10, pp. 2181–2195, 2017.
- [5] S. M. R. Islam, N. Avazov, O. A. Dobre, and K. Kwak, “Power-domain non-orthogonal multiple access (NOMA) in 5G systems: Potentials and challenges,” *IEEE Communications Surveys & Tutorials*, vol. 19, no. 2, pp. 721–742, 2017.
- [6] W. Shin, M. Vaezi, B. Lee, D. J. Love, J. Lee, and H. V. Poor, “Non-orthogonal multiple access in multi-cell networks: Theory, performance, and practical challenges,” *IEEE Communications Magazine*, vol. 55, no. 10, pp. 176–183, 2017.
- [7] M. Vaezi, R. Schober, Z. Ding, and H. V. Poor, “Non-orthogonal multiple access: Common myths and critical questions,” *IEEE Wireless Communications*, vol. 26, no. 5, pp. 174–180, 2019.
- [8] O. Maraqa, A. S. Rajasekaran, S. Al-Ahmadi, H. Yanikomeroglu, and S. M. Sait, “A survey of rate-optimal power domain NOMA with enabling technologies of future wireless networks,” *IEEE Communications Surveys & Tutorials*, vol. 22, no. 4, pp. 2192–2235, 2020.
- [9] L. You and D. Yuan, “A note on decoding order in user grouping and power optimization for multi-cell NOMA with load coupling,” *IEEE Transactions on Wireless Communications*, vol. 20, no. 1, pp. 495–505, 2021.
- [10] P. Xu, Z. Ding, X. Dai, and H. V. Poor, “A new evaluation criterion for non-orthogonal multiple access in 5G software defined networks,” *IEEE Access*, vol. 3, pp. 1633–1639, 2015.
- [11] J. Zhu, J. Wang, Y. Huang, S. He, X. You, and L. Yang, “On optimal power allocation for downlink non-orthogonal multiple access systems,” *IEEE Journal on Selected Areas in Communications*, vol. 35, no. 12, pp. 2744–2757, 2017.

- [12] M. S. Ali, E. Hossain, A. Al-Dweik, and D. I. Kim, "Downlink power allocation for CoMP-NOMA in multi-cell networks," *IEEE Transactions on Communications*, vol. 66, no. 9, pp. 3982–3998, Sept. 2018.
- [13] W. U. Khan, F. Jameel, T. Ristaniemi, S. Khan, G. A. S. Sidhu, and J. Liu, "Joint spectral and energy efficiency optimization for downlink NOMA networks," *IEEE Transactions on Cognitive Communications and Networking*, vol. 6, no. 2, pp. 645–656, 2020.
- [14] M. S. Ali, H. Tabassum, and E. Hossain, "Dynamic user clustering and power allocation for uplink and downlink non-orthogonal multiple access (NOMA) systems," *IEEE Access*, vol. 4, pp. 6325–6343, 2016.
- [15] S. Boyd and L. Vandenberghe, *Convex Optimization*. Cambridge University Press, 2009.
- [16] D. Tse and P. Viswanath, *Fundamentals of Wireless Communication*. Cambridge University Press, 2005.
- [17] R. D. Yates, "A framework for uplink power control in cellular radio systems," *IEEE Journal on Selected Areas in Communications*, vol. 13, no. 7, pp. 1341–1347, 1995.
- [18] Y. Fu, Y. Chen, and C. W. Sung, "Distributed power control for the downlink of multi-cell NOMA systems," *IEEE Transactions on Wireless Communications*, vol. 16, no. 9, pp. 6207–6220, 2017.
- [19] J. Cui, Y. Liu, Z. Ding, P. Fan, and A. Nallanathan, "QoE-based resource allocation for multi-cell NOMA networks," *IEEE Transactions on Wireless Communications*, vol. 17, no. 9, pp. 6160–6176, 2018.
- [20] L. You, D. Yuan, L. Lei, S. Sun, S. Chatzinotas, and B. Ottersten, "Resource optimization with load coupling in multi-cell NOMA," *IEEE Transactions on Wireless Communications*, vol. 17, no. 7, pp. 4735–4749, 2018.
- [21] D. Ni, L. Hao, Q. T. Tran, and X. Qian, "Transmit power minimization for downlink multi-cell multi-carrier NOMA networks," *IEEE Communications Letters*, vol. 22, no. 12, pp. 2459–2462, 2018.
- [22] L. Lei, L. You, Y. Yang, D. Yuan, S. Chatzinotas, and B. Ottersten, "Load coupling and energy optimization in multi-cell and multi-carrier NOMA networks," *IEEE Transactions on Vehicular Technology*, vol. 68, no. 11, pp. 11 323–11 337, 2019.
- [23] Y. Sun, D. W. K. Ng, Z. Ding, and R. Schober, "Optimal joint power and subcarrier allocation for full-duplex multicarrier non-orthogonal multiple access systems," *IEEE Transactions on Communications*, vol. 65, no. 3, pp. 1077–1091, 2017.
- [24] J. Zhao, Y. Liu, K. K. Chai, A. Nallanathan, Y. Chen, and Z. Han, "Spectrum allocation and power control for non-orthogonal multiple access in HetNets," *IEEE Transactions on Wireless Communications*, vol. 16, no. 9, pp. 5825–5837, 2017.
- [25] Z. Yang, C. Pan, W. Xu, Y. Pan, M. Chen, and M. Elkashlan, "Power control for multi-cell networks with non-orthogonal multiple access," *IEEE Transactions on Wireless Communications*, vol. 17, no. 2, pp. 927–942, 2018.
- [26] K. Wang, Y. Liu, Z. Ding, A. Nallanathan, and M. Peng, "User association and power allocation for multi-cell non-orthogonal multiple access networks," *IEEE Transactions on Wireless Communications*, vol. 18, no. 11, pp. 5284–5298, 2019.
- [27] A. B. M. Adam, X. Wan, and Z. Wang, "Energy efficiency maximization in downlink multi-cell multi-carrier NOMA networks with hardware impairments," *IEEE Access*, vol. 8, pp. 210 054–210 065, 2020.
- [28] C. Liu and D. Liang, "Heterogeneous networks with power-domain NOMA: Coverage, throughput, and power allocation analysis," *IEEE Transactions on Wireless Communications*, vol. 17, no. 5, pp. 3524–3539, 2018.
- [29] A. Zappone, E. Björnson, L. Sanguinetti, and E. Jorswieck, "Globally optimal energy-efficient power control and receiver design in wireless networks," *IEEE Transactions on Signal Processing*, vol. 65, no. 11, pp. 2844–2859, 2017.
- [30] S. Rezvani and E. A. Jorswieck, "Optimal SIC ordering and power allocation in downlink multi-cell NOMA systems," <https://gitlab.com/sepehrrezvani/Optimal-JSPA-MultiCell-NOMA.git>, 2021.